Hochschule
Bonn-Rhein-Sieg
University of Applied Sciences

b-it Bonn-Aachen International Center for Information Technology

R&D Project

Semantic Segmentation using Resource Efficient Deep Learning

Naresh Kumar Gurulingan

Submitted to Hochschule Bonn-Rhein-Sieg,
Department of Computer Science
in partial fullfilment of the requirements for the degree
of Master of Science in Autonomous Systems

Supervised by

Prof. Dr Paul G. Plger
M. Sc. Deebul Nair

August 2018

I, the undersigned below, declare that this work has not previously been submitted to this or any other university and that it is, unless otherwise stated, entirely my own work.

Date	Naresh Kumar Gurulingan

Abstract

Your abstract

Acknowledgements

Thanks to ....

Contents

1

Introduction

In recent years, deep learning has significantly impacted research in the field of computer vision. Variations of Convolutional Neural Network architectures have shown state-of-the-art performance in computer vision tasks such as image classification [5], object detection [8], action recognition [10] and semantic segmentation [4]. A considerable part of this success comes from the supervised learning paradigm through which the networks are trained with labeled samples.

State-of-the-art deep learning techniques in semantic segmentation also make use of the supervised learning paradigm. Semantic segmentation is treated as a pixelwise classification problem with the goal of assigning a class from a list of desired classes to every pixel in an image. The resultant image splits objects of interest into different regions thereby achieving the intended segmentation in a meaningful manner.

1.1 Motivation

Semantic segmentation is a rich source of information

1.1.1 ...

1.1.2 ...

1.2 Challenges and Difficulties

1.2.1 ...

1.2.2 ...

1.2.3 ...

1.3 Problem Statement

1.3.1 ...

1.3.2 ...

1.3.3 ...

2

State of the Art

2.1 ....

Use as many sections as you need in your related work to group content into logical groups

Don't forget to correctly cite your sources [6].

2.2 Limitations of previous work

3

DCNN and Semantic Segmentation

3.1 What is semantic segmentation

3.2 Traiditional methods

3.3 Deep Learning for Semantic Segmentation

3.4 Artificial Neural Networks

3.5 Convolutional Neural Networks

4

Dataset creation

4.1 Overview of the dataset

Since semantic segmentation using deep learning is framed as a pixelwise classification task, an image of dimensions H×W×C requires a ground truth of dimensions H×W, where H and W are the height and width of the image in the dataset having C number of channels.

The scope of the dataset is to include objects associated to RoboCup @Work. The selected 18 objects are shown in Figure 4.1.

Each of the objects were taken individually, placed on 3 different backgrounds and 30 images were taken. This lead to a total of 540 images which were to be manually labeled. Since, every pixel of the images needs to be labeled, the process of manual annotation would be time consuming. Therefore, a decision was made to first annotate the 540 images and later decide whether more images could be taken based on the effort required for annotation.

4.2 Selection of a labeling tool

In order to reduce the time required to annotate an image, it was imperative to select a tool which is specifically designed for semantic segmentation and also provides algorithms which helps the annotator by providing labeling automation to the highest possible extent.

The following available tools were evaluated for ease of use and time taken for annotation:

(a) axis [1]

(b) bearing [1]

(c) bearing box AX01 [1]

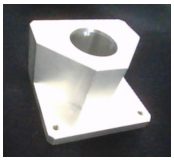

(d) bearing box AX16

(e) container blue [1]

(f) container red [1]

(g) distance tube [1]

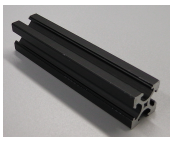

(h) F20_20_B [1]

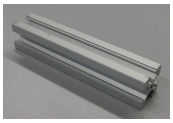

(i) F20_20_G [1]

(j) M20 [1]

(k) M20_100 [1]

(l) M30 [1]

(m) motor [1]

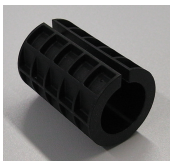

(n) R20 [1]

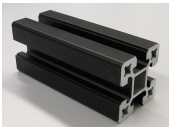

(o) S40_40_B [1]

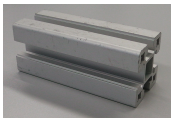

(p) S40_40_G [1]

(q) em_01

(r) em_02

Figure 4.1: Different objects required in the dataset

- LabelMe: web based tool is public and data would also be public.
- LabelMe Matlab toolbox: yet to try..
- University bonn annotation tool:
- Pixel annotation tool (using watershed algorithm): works in windows. Seems to be useful.
- Ratsnake: tool dint seem to be useful although the website had options like superpixel suggestions.
- LabelImg: Can be used but time consuming.
- Figi: used in medical image segmentation. Has many options. Still exploring.
- Supervisely.
- MATLAB ImageLabeler available in release R2017b (Computer Vision Toolbox).

4.3 Description of the labeling process

MATLAB ImageLabeler was used for the labeling process. At first, label definitions are created and exported to a .mat file. This file is used to load label definitions for all images to maintain consistency of labels. The contents of the .mat file is shown in the Figure 4.2a.

The ImageLabeler app, by default, provides different tools which help create pixelwise labels. The tools are shown in the Figure 4.3. These tools become accessible once an image and the label definitions are loaded. A short description of the tools is given below:

- Polygon: This can be used to trace an object boundary by placing dots. Once a closed contour is created, pixels within the contour get assigned the corresponding object label.
- Smart Polygon: Can be used in a similar fashion like the Polygon tool. This tool, in addition, tries to reach out to the nearby edges of the drawn polygon.

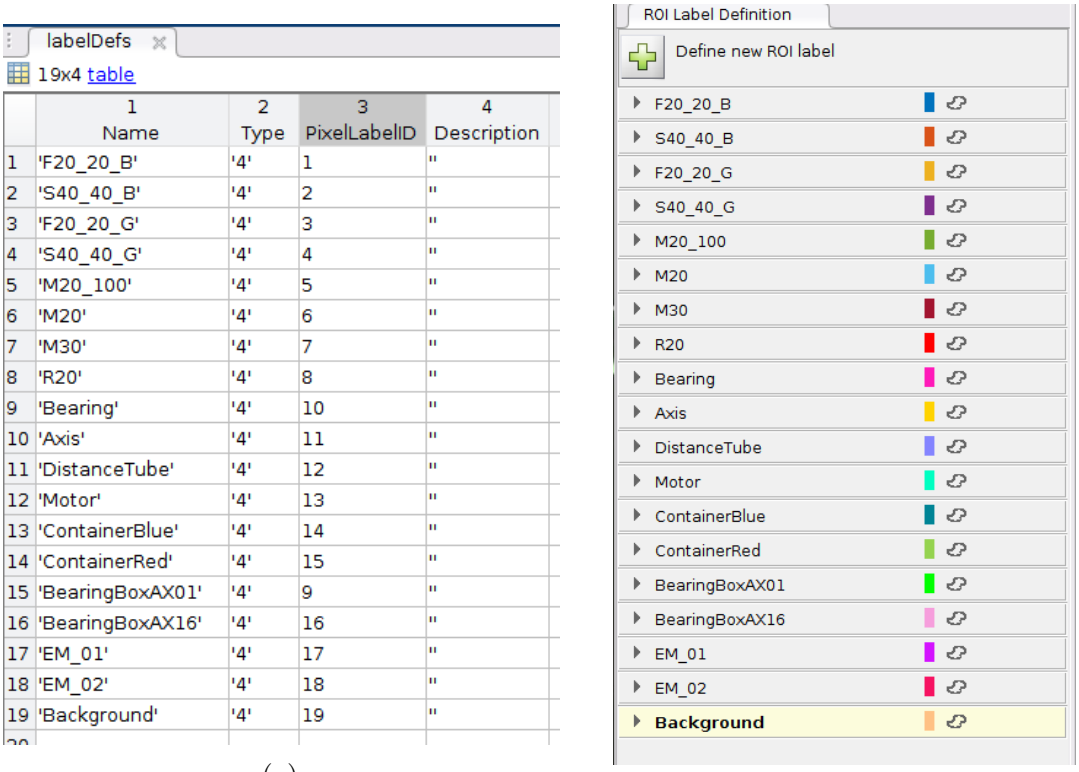

	1 Name	2 Type	3 PixelLabelID	4 Description
1	'F20_20_B'	'4'	1	''
2	'S40_40_B'	'4'	2	''
3	'F20_20_G'	'4'	3	''
4	'S40_40_G'	'4'	4	''
5	'M20_100'	'4'	5	''
6	'M20'	'4'	6	''
7	'M30'	'4'	7	''
8	'R20'	'4'	8	''
9	'Bearing'	'4'	10	''
10	'Axis'	'4'	11	''
11	'DistanceTube'	'4'	12	''
12	'Motor'	'4'	13	''
13	'ContainerBlue'	'4'	14	''
14	'ContainerRed'	'4'	15	''
15	'BearingBoxAX01'	'4'	9	''
16	'BearingBoxAX16'	'4'	16	''
17	'EM_01'	'4'	17	''
18	'EM_02'	'4'	18	''
19	'Background'	'4'	19	''

(a) (b)

Figure 4.2: (a) Contents of the labelDefs .mat file, (b) ROI Label Definitions window.

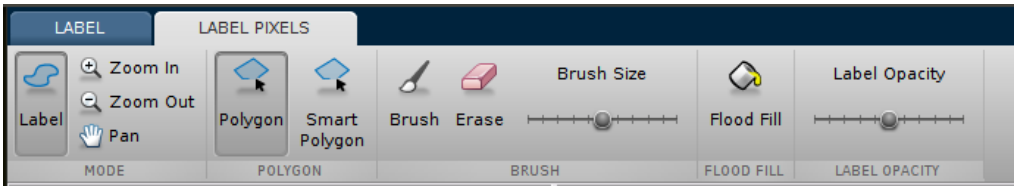

Figure 4.3: Tools provided by the ImageLabeler app

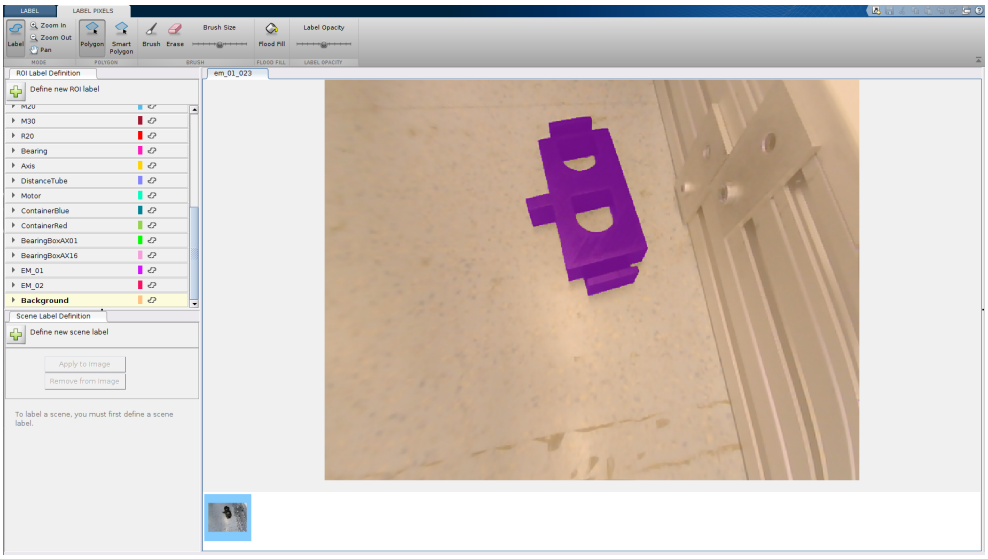

Figure 4.4: An object labeled in the ImageLabeler.

- Brush and Erase: Square shaped brush and eraser to either label a region or remove labels from a region. The size of the square can be changed by using the Brush Size slider.
- Flood Fill: This tool provides same labels to pixels which are similar in terms of the intensity with the selected pixel.
- Label Opacity: This tool provides a sliding bar which varies the opacity of the overlayed labels on the image. This is helpful to visualize the assigned labels.
- Zoom In, Zoom Out, Pan: These tools improve the ease of labeling by providing means to focus on particular regions by zooming and panning.

The ImageLabeler app by default assigns different colors to different objects to aid visualization. The label colors are shown in the ROI Label Definition window shown in Figure 4.2b. An example of an object in the ImageLabeler tool once the annotation is complete is shown in Figure 4.4.

The ImageLabeler app does not provide any tool to label all unlabeled pixels as background. In order to save time, the following workarounds have been used:

- The images taken for the dataset each have only one object in them.

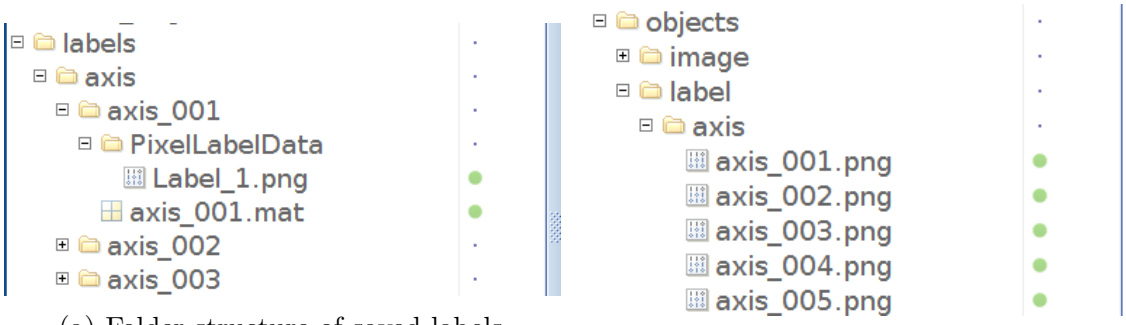

(a) Folder structure of saved labels

(b) Rearranged folder structure

Figure 4.5: Different folder structures

- Only the object region is labeled.
- Since the ImageLabeler app does not provide any tool to label all unlabeled pixels as background, a python code which simply reads the label image and replaces unlabeled values 0 with background label value 19, was used for this purpose. The code is also used to double check the label image in order to avoid noisy labeling.

The Export Labels –> To File option can be used to save the annotations. This is done for all images individually to arrive at the folder structure shown in Figure 4.5a.

The saved .mat file can be loaded into ImageLabeler again to further modify labels if required later. The 'Label_1.png' file located in the PixelLabelData folder (as can be seen in Figure 4.5a) is the label image. This image is renamed to have the same name as the image file and a folder structure as in Figure 4.5b is created by using a python code.

The final folder structure is shown in Figure 4.6. The image folder and label folder are similar and contain object images and corresponding label images with same names.

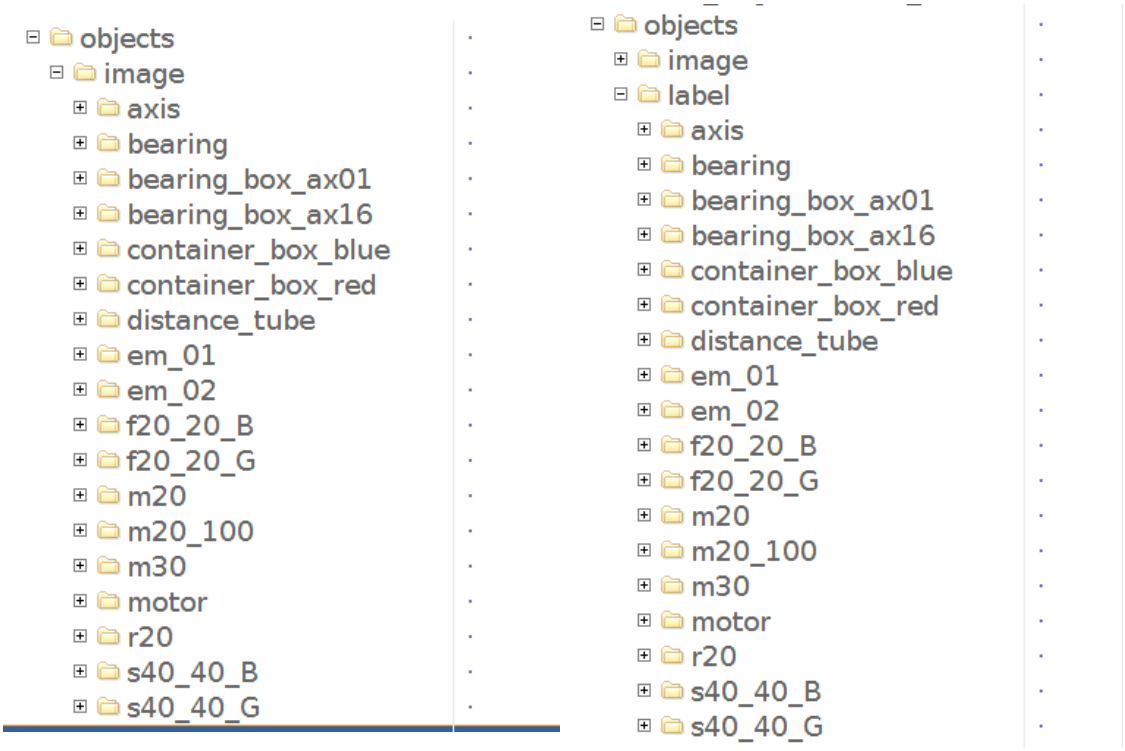

Figure 4.6: Folder structure showing different object folders in both image and label folders.

4.4 Artificial image generation algorithm

4.4.1 Motivation

- Manually labeling 540 images with the described process in Section 4.3 takes roughly 2160 minutes (roughly 4 minutes per image). This is equivalent to around 4 working days. Hence, creating a large dataset with manual labeling is not feasible.
- Taking images in a variety of real world backgrounds is also time consuming.
- Labeling images with multiple objects would take an even longer time.

These drawbacks could be overcome by randomly placing objects on a variety of different background images automatically using an algorithm.

4.4.2 Process of artificial image generation

The artificial image generation algorithm requires that every image provided must have just one object. The algorithm can be used in two modes named "Generate artificial images" and "Save visuals". The first mode can be used to generate artificial images and if required save visualizations of labels. The second mode can be used to just save visualizations. Under the first mode, the entire process can be divided into 7 broad steps:

1 **External interface**: An interface to obtain possible parameters to control the generation process. These parameters are obtaiend through argparse command line GUI and are called generator options.

2 **Get backgrounds and data**: Fetch all the backgrouds, images and corresponding labels from the provided respective background, image and label paths. First, all the images in the backgrounds path are read. Then, all available images in the label path is read and the corresponding image files in the provided image path is read. The images in the image path must have the same name as that of the corresponding labels but can be of a different format. The default image format is ".jpg".

3 **Get object details**: Fetch details regarding every object and its different scales. The details include information regarding object locations in an image, object values, label values, the object name, points in pixel space denoting a bounding rectangle around the object, and object area. The scales for every object is determined at random. Scaled objects which are too small or too big as determined by generator options are removed.

4 **Generate augmenter list**: Every element in the augmenter list denotes an artificial image and contains information including the chosen background image, the number of objects to place in the artificial image, which objects from the object details list are selected and locations in pixel space where the selected objects need to be placed. In this stage, elements which are cluttered with too many objects are removed as determined by the generator options.

5 **Generate artificial images**: Based on every element in the augmenter list, artificial images and corresponding labels are generated. Every element is taken one by one. The selected objects are placed on the selected background in the corresponding specified location, one by one. The resultant artificial image and semantic label is saved in the directory specified using generator options. Additionally, object detection labels, semantic masks and visualization previews can be saved by configuring generator options.

6 **Visualize results**: The generated images and labels are visualized to verify the generation process.

7 **Save results**: The obtained resultant artificial images, corresponding labels and generated visualizations are saved.

Under the second mode, steps 3 to 6 in the above process is skipped. Step 2 fetches also the object detection labels in addition to the image and semantic labels. Step 7 saves the visualizations of read image, semantic labels and object detection labels.

4.4.3 Generator options

A number of arguments can be configured to control the generation process. Configuration of generator options is possible through command line GUI. Details regarding the arguments are provided in Table 4.1 and in Table 4.2.

4.4.4 Sample results

Sample results of the artificial image generation algorithm can be seen in Figure 4.7. These images are generated using different backgrounds and hence the dataset is referred to as variety of backgrounds dataset. The bounding box in the label visualization image represents the object detection label and the different colors of the segmentation labels denote different label values. The colors were chosen in such a way that they are as distinct from each other as possible [3].

4.4.5 Downloading background images

Different background images were used for the artificial image generation process. Since a large number of backgrounds were required, manual download was time consuming. Hence, the "google-images-download" [2] script was used to auto download images. The search keywords used to obtain the background images are listed in Table 4.3. From the downloaded images, the required number of images for each dataset split were selected. For the white backgrounds dataset, many different search keywords were tried as is evident from the Table 4.3. This was because many of the downloaded images did not contain sufficient white regions. Images which were not of the dimensions used in the dataset (480×640) were rescaled.

4.4.6 Notable features of the artificial image generator

In this section, certain features of the artificial image generator which are noteworthy are listed.

- The generator automatically creates object detection labels in addition to semantic labels. The object detection labels are obtained by finding the

Generator options	Description
mode	1: Generate artificial images; 2: Save visuals.
image_dimension	Dimension of the real images.
num_scales	Number of scales including original object scale.
backgrounds_path	Path to directory where the background images are located.
image_path	Path to directory where real images are located.
label_path	Path to directory where labels are located.
obj_det_label_path	Path to directory where the object detection csv labels are located.
real_img_type	The format of the real image.
min_obj_area	Minimum area in percentage allowed for an object in image space.
max_obj_area	Maximum area in percentage allowed for an object in image space.
save_label_preview	Save image+label in single image for preview.
save_obj_det_label	Save object detection labels in csv files.
save_mask	Save images showing the segmentation mask.
save_overlay	Save segmentation label overlaid on image.
overlay_opacity	Opacity of label on the overlaid image.
image_save_path	Path where the generated artificial image needs to be saved.
label_save_path	Path where the generated segmentation label needs to be saved.
preview_save_path	Path where object detection labels needs to be saved.
obj_det_save_path	Path where object detection labels needs to be saved.
mask_save_path	Path where segmentation masks needs to be saved.
overlay_save_path	Path where overlaid images needs to be saved.
start_index	Index from which image and label names should start.
name_format	The format for image file names.
remove_clutter	Remove images cluttered with objects.
num_images	Number of artificial images to generate.
max_objects	Maximum number of objects allowed in an image.
num_regenerate	Number of regeneration attempts of removed details dict.
min_distance	Minimum pixel distance required between two objects.
max_occupied_area	Maximum object occupancy area allowed.
scale_ranges	Can be used to change the zoom range of specific objects.

Table 4.1: Description of generator options

Generator options	Default value	Is required?
mode	1	Not required
image_dimension	[480, 640]	Not required
num_scales	'randomize'	Not required
backgrounds_path	None	Required if mode is 1
image_path	-	Required
label_path	-	Required
obj_det_label_path	None	Required if save_label_preview is True and mode is 2
real_img_type	'.jpg'	Not required
min_obj_area	20	Not required
max_obj_area	70	Not required
save_label_preview	False	Not required
save_obj_det_label	False	Not required
save_mask	False	Not required
save_overlay	False	Not required
overlay_opacity	0.6	Not required
image_save_path	None	Required if mode is 1
label_save_path	None	Required if mode is 1
preview_save_path	None	Required if save_label_preview is True
obj_det_save_path	None	Required if save_obj_det_label is True
mask_save_path	None	Required if save_mask is True
overlay_save_path	None	Required if save_overlay is True
start_index	0 if mode is 1 " if mode is 2	Not required
name_format	'%05d'	Not required
remove_clutter	True	Not required
num_images	20	Not required
max_objects	10	Not required
num_regenerate	100	Not required
min_distance	100	Not required
max_occupied_area	0.8	Not required
scale_ranges	None	Not required

Table 4.2: Default value of generator options and whether the options are required to be set.

Figure 4.7: Sample results produced by the artificial image generation algorithm for the variety of backgronds dataset. In each row, the image on the left shows the generated artificial image and the image on the right shows a visualization of the semantic segmentation label and object detection label. At the top of every label visualization image, the objects in the image and their corresponding colors in the visualization are indicated.

Used in	Search keyword(s)	Number of images selected
Training set	640x480 background images, 640x480 textures images, 640x480 wallpapers	150
Validation set	640x480 abstract	25
Test set	640x480 paintings	25
Shades of white	640x480 white abstract, 640x480 white backgrounds, 640x480 white textures, 640x480 white wallpaper, light gray, white, white clouds, white floors, white frost, white mist, white pebbles, white snow, white table textures	150

Table 4.3: This table lists the keywords used to download images used as background for artificial image generation.

rectangle points which describe a bounding rectangle around the semantic labels.

- The generated artificial images and labels can be visualized in three different ways. A preview which shows the image alongside the generated labels. A mask image showing the different classes in different colors. An overlay image in which the generated labels are overlayed on top of the corresponding generated images. The opacity of overlay can be configured through generator options. Examples of visualizations can be seen in Figure 4.8 and in Figure 4.7.

4.4.7 Artificial images for each dataset split

The real images are split into training, validation and test sets. Real images in each of these sets are used to generate artificial images for the coresponding set. This ensures that the final training, validation and test sets are different from each other. The scale range of distance_tube was set to 1.1 to 2.0 for generating training artificial images and to 0.6 to 1.2 for generating validation and test artificial images.

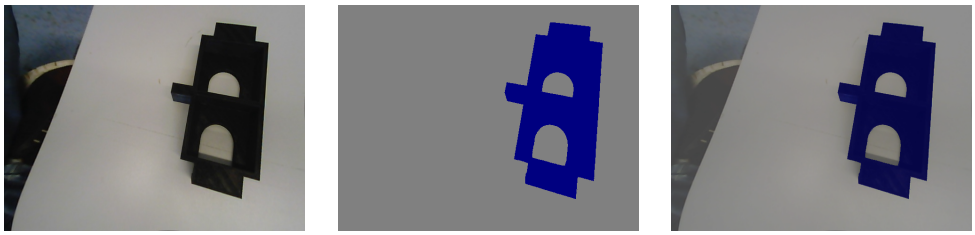

(a) Image containing object em_01

(b) Corresponding segmentation mask

(c) Corresponding overlay visualization

Figure 4.8: This figure shows examples of two different types of visualization, "mask" and "overlay". The third type "preview" can be seen in figure 4.7

The reason for this setting is provided in the data analysis section 4.6.

4.5 Creation of dataset variants:

Different variants of the dataset are created based on the properties of the objects in the dataset, and the type of background images used for generation of artificial images.

4.5.1 Motivation

Looking into the objects present in the dataset, it is apparant that some objects are similar in certain aspects. For instance, the objects m20 and m30 are very similar to each other except that m30 is bigger in size and has a slightly different color. Because of the similarities existing among objects, the segmentation model could face certain difficulties as listed below:

- **Inability to distinguish size**: The segmentation model is given no information regarding the positions of the camera or the object in the real world. If camera extrinsic calibration information is available to the segmentation model, the model could possibly learn to distinguish different sizes. However, such information is not available. In addition, the objects in the artificial images are randomly scaled to different sizes thereby removing any size related information available.

- **Inability to distinguish subtle variations in color**: The real images were taken under different lighting conditions. As a result, there is no consistent

(a) A viewpoint of bearing box ax01

(b) A viewpoint of bearing box ax16

Figure 4.9: A similar viewpoint of bearing box ax01 and bearing box ax16 where the difference in shapes between the two objects is clearly visible.

(a) A viewpoint of bearing box ax01

(b) A viewpoint of bearing box ax16

Figure 4.10: A similar viewpoint of bearing box ax01 and bearing box ax16 where the appear similar in shape.

difference in color information available between classes. This makes it difficult for the segmentation model to learn patterns in color information.

- **Inability to distinguish shapes**: Certain objects are closly related to each other in terms of shape and differ only slightly. For instance, bearing_box_ax16 and bearing_box_ax01 are similar in shape except in a few viewpoints as illustrated in Figure 4.9 and in Figure 4.10. In such cases, in certain viewpoints, the segmentation model would not be able to distinguish between similarly shaped objects.

4.5.2 Dataset variants

Four different dataset variants have been created as listed below:

- **atWork_full**: This variant has different label values for all the 18 objects in the dataset and an additional label value for background. The total number

of classes is 19 including background and the label values range from 0 to 18. The different classes in this variant along with their label values are listed in Table 4.4.

- **atWork_size_invariant**: In this variant, objects which are similar to each other in terms of shape but differ in size are combined together into one class. On this regard, f20_20_B and s40_40_B are combined and named f_s20_40_20_40_B. Similarly, f20_20_G and s40_40_G are combined and named f_s20_40_20_40_G. m20 and m30 are combined and named m20_30. The two bearing boxes, bearing_box_ax01 and bearing_box_ax16 are also combined together as they are similar to each other in certain viewpoints. They form the new class bearing_box. The objects in this variant along with their label values are listed in Table 4.4. This variant is named "atWork_size_invariant" as in this variant, the major change deals with the ignorance of the size of the objects as distinguishing information.

- **atWork_similar_shapes**: In the previous variant "atWork_size_invariant", objects similar in terms of shape but different in terms of color were treated as separate classes. In this variant, variation in terms of color is also ignored. In addition to the previous variant, f_s20_40_20_40_B and f_s20_40_20_40_G are combined and named f_s20_40_20_40_B_G. The container boxes, container_box_red and container_box_blue were also combined to form the new class container_box. This variant is named "atWork_similar_shapes" as objects with similar shapes are given equal label values. Details regarding this variant are listed in Table 4.4.

- **atWork_binary**: An interesting question would be, "how would a segmentation model perform when it is just tasked with segmenting foreground from background". To address this question, an additional variant is created called "atWork_binary" where are the objects of interest are combined to form the "foreground" class with label value 1. The "background" class retains its label value of 0. The classes in this variant are listed in Table 4.4.

Label Value	atWork_ full Objects	atWork_size_ invariant Objects	atWork_similar_ shapes Objects	atWork_ binary Objects
0	background	background	background	background
1	f20_20_B	f_s20_40_20_40_B	f_s20_40_20_40_B_G	foreground
2	s40_40_B	f_s20_40_20_40_G	m20_100	-
3	f20_20_G	m20_100	m20_30	-
4	s40_40_G	m20_30	r20	-
5	m20_100	r20	bearing_box	-
6	m20	bearing_box	bearing	-
7	m30	bearing	axis	-
8	r20	axis	distance_tube	-
9	bearing_box_ax01	distance_tube	motor	-
10	bearing	motor	container	-
11	axis	container_box_blue	em_01	-
12	distance_tube	container_box_red	em_02	-
13	motor	em_01	-	-
14	container_box_blue	em_02	-	-
15	container_box_red	-	-	-
16	bearing_box_ax16	-	-	-
17	em_01	-	-	-
18	em_02	-	-	-

Table 4.4: Details of the "atWork_full" variant

4.5.3 White backgrounds dataset

The backgrounds used for the artificial image generation process are images with a variety of different colors, textures and so on. In essense, the background images do not seem to follow any pattern as such. As a result, the generated artificial images are unlikely to be similar to an image taken by an atWork robot. In order to address this, the background images used in the artificial image generation process are all replaced with images which mostly contain shades of white color in them. With this as the only change, the entire artificial image generation process and variant creation process is repeated to arrive at a new dataset which is named "white backgrounds dataset". Sample visualizations of artificial images generated for this dataset can be seen in 4.11.

4.6 Data analysis:

All the variants of the dataset are analyzed in terms of the pixels occupied by each class in percentage and the number of images in which each class appears.

4.6.1 Surface area of the objects

In order to comprehend the reasons as to why an object constitutes a certain percentage of pixels in a dataset split, the surface area of the objects in the real world could be considered. It is natural to assume that the percentage of pixels occupied by the objects is roughly proportional to the surface area of the object. However, not all objects have a strictly defined geometric shape. For this reason, the closest geometric shape to each object is assumed to calculate the surface area. The table provides details about the assumed geometric shapes and the surface areas for each object.

4.6.2 Analysis of "atWork_full" variant

The total pixels occupied by each class in each of the training, validation and test sets is calculated. Next, this count of pixels is converted to percentage with

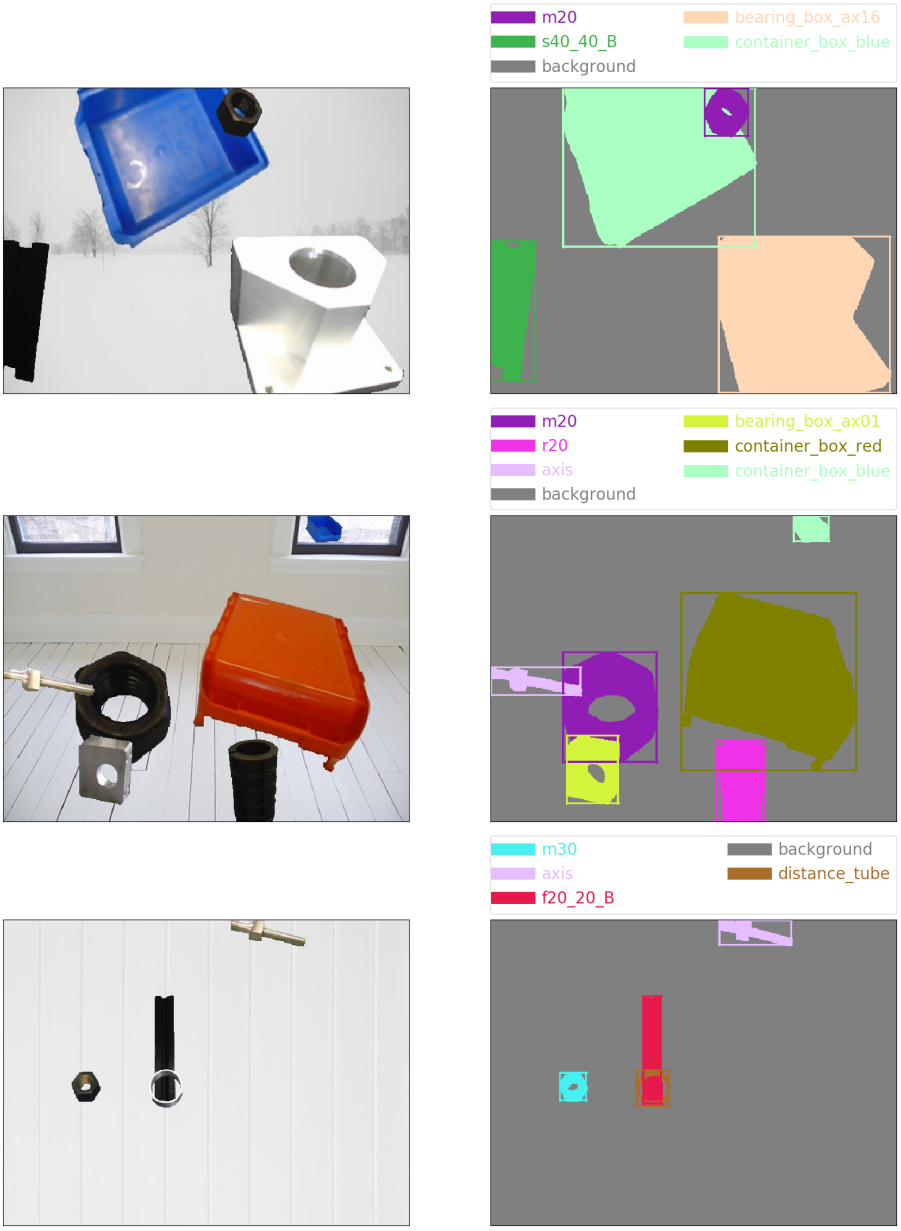

Figure 4.11: Sample results produced by the artificial image generation algorithm for the "white backgrounds dataset".

Object name	**Assumed shape**	**Surface area**
f20_20_B	cuboid	
s40_40_G	cuboid	
f20_20_G	cuboid	
s40_40_G	cuboid	
m20_100		
m20		
m30		
r20		
bearing_box_ax01		
bearing		
axis		
distance_tube		
motor		
container_box_blue		
container_box_red		
bearing_box_ax16		
em_01		
em_02		

Table 4.5: Assumed shape and surface area of objects

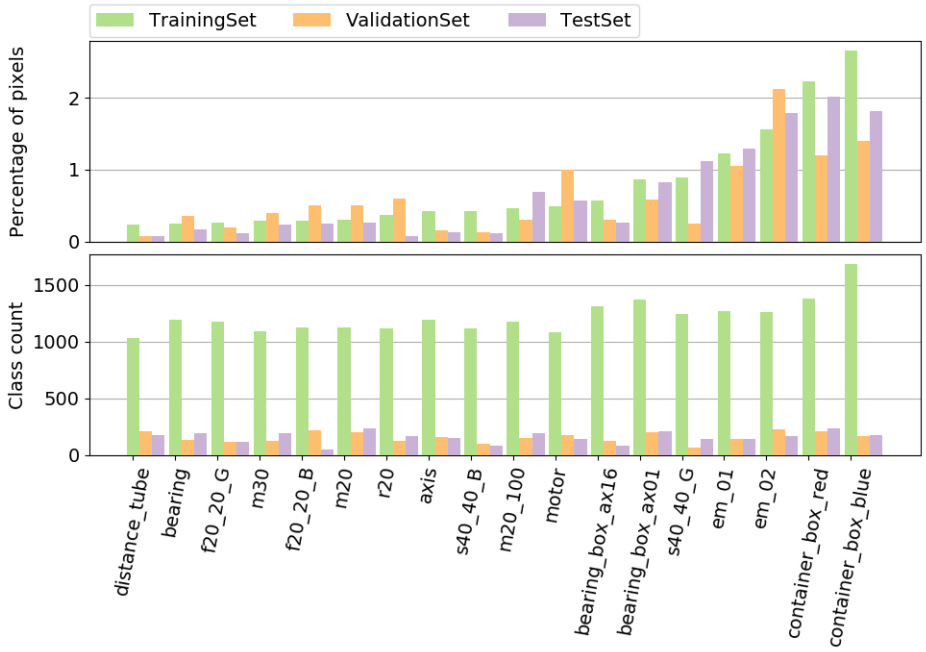

Figure 4.12: Percentage of pixels occupied by every class, except the background class, and corresponding class counts in the atWork_full variant. The larger objects such as "container_box_blue" occupy more number of pixels in comparision to smaller objects such as "distance_tube".

respect to the total number of pixels in the corresponding dataset split. Also, the number of images in which each class of objects appears is counted and called class count. The resulting plots are shown in **??** and 4.12. In **??**, it is evident that compared to the background class, the object classes occupy almost negligible pixel area. This is desired as the background class is present in all images and in most of them, occupies the most pixel area. The larger object classes occupy the most pixel area as can be seen in 4.12. However, in terms of class count all objects are fairly close to each other. A direct reason is infact that larger size occupies more pixel area. Indirectly however, the larger objects are less likely to be rejected by the artificial image generation algorithm after being randomly scaled. This again leads to increased pixel area occupied by the larger objects.

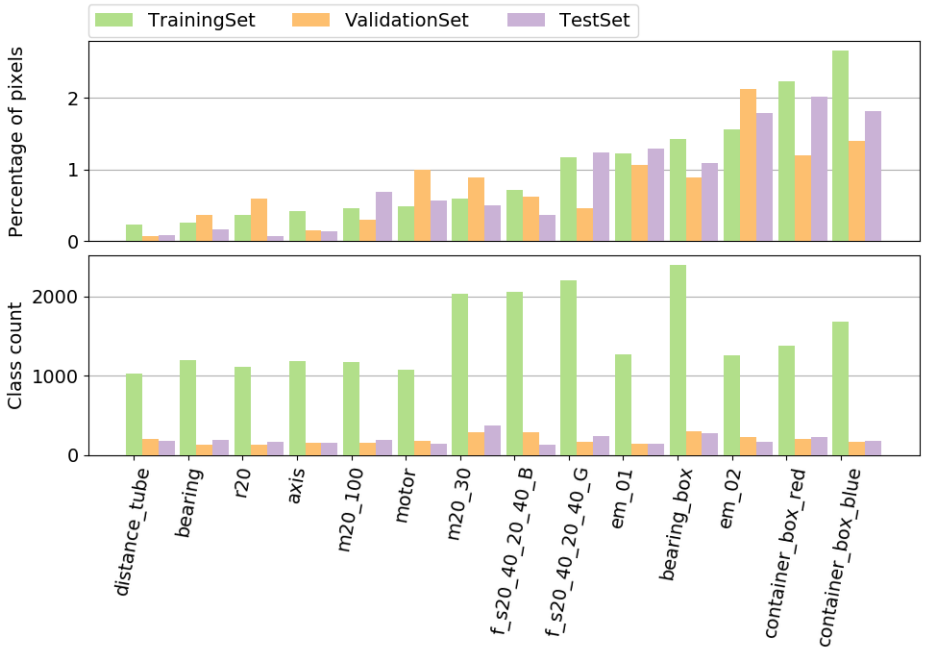

Figure 4.13: Percentage of pixels occupied by every class, except the background class, and corresponding class counts in the atWork_size_invariant variant.

4.6.3 Analysis of "atWork_size_invariant" variant

4.6.4 Analysis of "atWork_similar_shapes" variant

4.6.5 Analysis of "atWork_binary" variant

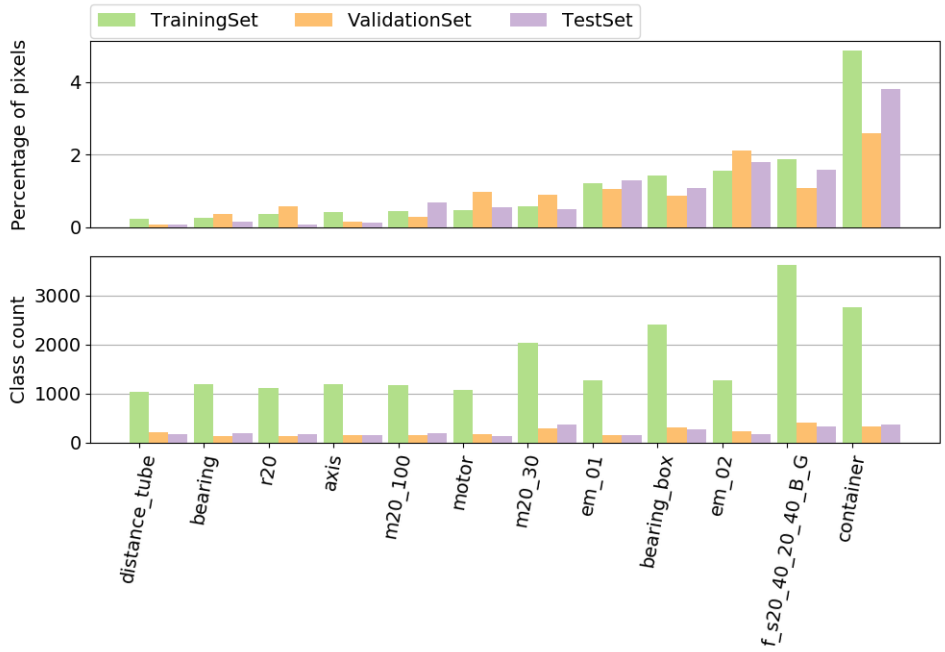

Figure 4.14: Percentage of pixels occupied by every class, except the background class, and corresponding class counts in the atWork_similar_shapes variant.

4.7 Meta-data of the dataset

Meta-data of the dataset is provided in table 4.6. These numbers hold true for all four dataset variants and also for the shades of white dataset. Initially, 30 images were captured for each of the 18 objects leading to a total of 540 images. However, 1 image of "axis" object and 2 images of "s40_40_B" were removed as they were blurred.

	Training	Validation	Test
Real Images	22 per object. Total: 22×18=396	4 per object. Total: 4×18=72	"axis"=3; "s40_40_B"=2; All other objects=4 Total: (4×18)-3=69
Augmented Images	7104	870	870
Total Images	7500	942	939

Table 4.6: Meta-data of all 4 variants and also the shades of white dataset.

4.8 Possible directions of improvement

Creating a custom dataset for a desired application is evidently challenging. To overcome the time consuming nature of creating annotations for semantic segmentation, choices such as 1. placing just 1 object per image while taking real images and 2. augmenting the objects on a random selection of diverse backgrounds, were made. This method of augmentation, although inspired by dataset generation method used in [7] and the Synthia dataset [9], takes a different approach. Unlike [7], which uses 3D CAD models, this approach does not require any 3D models. Also, this approach does not require a virtual world as used by the Synthia dataset [9]. However, the effectiveness of the dataset is yet to be verified by training and testing available segmentation models. The following list provides possible directions of improvement:

- The ImageLabeler app by default saves the label '.png' file with the name 'Label_1.png' in a folder called PixelLabelData. A automation script can be written and added to the ImageLabeler to provide options to save the label file in a way the user wants.
- Creating a way to replace all unlabeled pixels with the label value of 'background' from within the ImageLabeler would be helpful. For now, this is done by first exporting the label, then loading the label using opencv in python to replace 0 (value of unlabeled pixels) with 19 (value of 'background').
- The augmentation script is written in python and is independent of the MATLAB ImageLabeler app. This can be improved by including a way to start augmentation right from the ImageLabeler.

5

Methodology

In line with the goal of the project to use resource efficient deep learning in terms of inference time and storage memory, the deepLab v3+ model with mobileNetv2 and xception variant was chosen. In order to better understand deepLabv3+, we consider breaking down the architectures of the previous versions of deepLab leading upto the current version. The different versions of deepLab are deepLab, deepLabv2, deepLabv3 and deepLabv3+ (the current version also called as deepLabv4). Also, we review the pruning and quantization methods considered for this work.

5.1 DeepLab

Fully Convolutional networks were introduced by [] for the task of semantic segmentation. The predictions obtained with the help of this network were coarse and the object boundaries were not sufficiently delineated. In order to overcome these difficulties, the authors of deepLab proposed the use of atrous convolutions and fully-connected Conditional Random Fields (CRF).

Atrous convolutions, also called as dilated convolutions, is be used to gather a better global context with enlarged field-of-view on the feature maps. A atrous rate called r, determines the field-of-view of an atrous convolution. With increase in dilation rate, a greater region in the feature map is convolved over. This leads to gathering of more global context. However, it is worth noting that there is no increase in the number of parameters in the convolution filter. Only the convolved

region in the input feature map changes. When the dilation rate is 1, usual convolution is performed. The figure 5.1 illustrates atrous convolution.

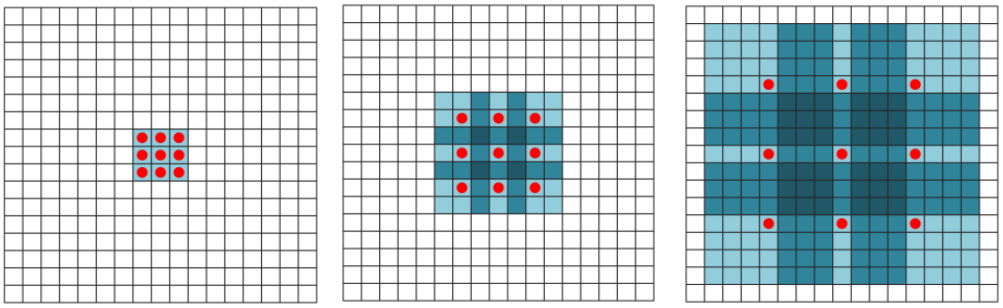

(a) Atrous rate = 1 (b) Atrous rate = 2 (c) Atrous rate = 3

Figure 5.1: Illustration of atrous convolution with three different atrous rates.

Fully-connected Conditional Random Fields (CRF), is used to post process the prediction of the CNN to improve object delineation. Every pixel in the output feature map is connected to every other pixel resulting in pairwise terms. In each pairwise term, based on color and position, the similarity between pixels is determined and a class is assigned for the pixels.

5.2 DeepLabv2

In DeepLabv2, Atrous Spatial Pyramid Pooling (ASPP) was used in addition to the existing architecture. The authors also use deeper ResNet network to improve accuracy.

Atrous Spatial Pyramid Pooling, is used to create multiscale feature representations. Atrous convolutions with different atrous rates are applied to the same feature map. The resulting feature maps from each atrous convolution is processed in separate branches in a similar fashion as in deepLabv1 by using two 1×1 convolutions. Each of the branches are then fused together to obtain multi-scale information. The difference between in architecture between deepLabv1 and deepLabv2 is illustrated in 5.3.

5.3 DeepLabv3

In this version of deepLab, the contributions include improvements to the context module, and the use of batch normalization. Batch Normalization is

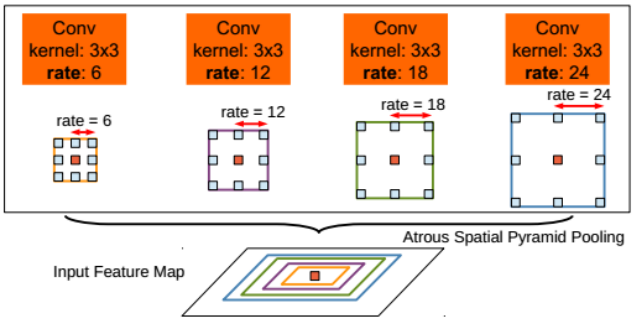

Figure 5.2: Illustration of Atrous Spatial Pyramid Pooling (ASPP). Atrous convolutions with 4 different rates convolve on the same input feature map. The field-of-view of each atrous rate is shown using different colors.

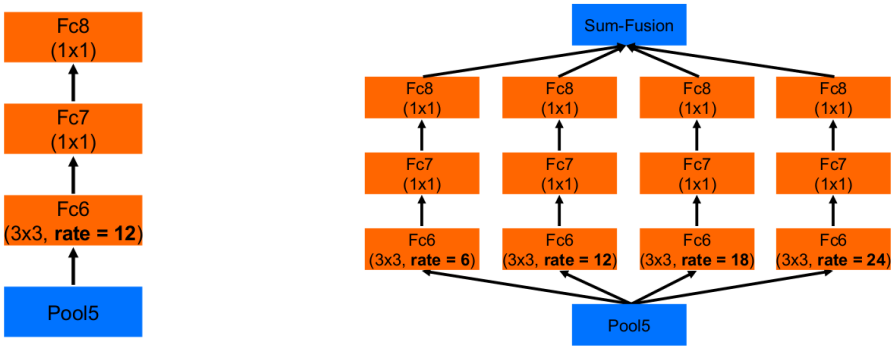

(a) Large field-of-view in DeepLabv1

(b) ASPP in DeepLabv2

Figure 5.3: Illustration of the difference in architecture between DeepLabv1 and DeepLabv2.

applied to every layer in the context module and the parameters of the batch normalization layers are trained.

The authors experiment with two different modules to handle context one being a cascade module and the other being an improved version of ASPP module. The cascade module is formed by repeating the last block from ResNet and replacing convolutions with atrous convolutions. The authors report that performing this repetition upto three times improves performance. The cascade module is illustrated in 5.4a. The ASPP module used in deepLabv3 is similar to the one used in deepLabv2. However, the difference now is that the ASPP module uses five branches. The first four branches perform 1×1 convolution, and three 3×3

convolutions with atrous rates 6, 12 and 18. The 5th branch provides image level features by performing global average pooling on the last feature maps of the model. The resulting channels are concatenated and projected to a different channel space using 1×1 convolution.

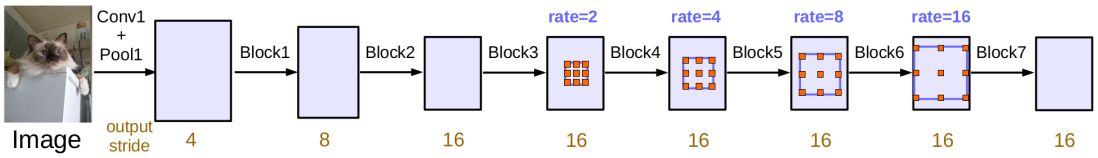

(a) cascade module in DeepLabv3

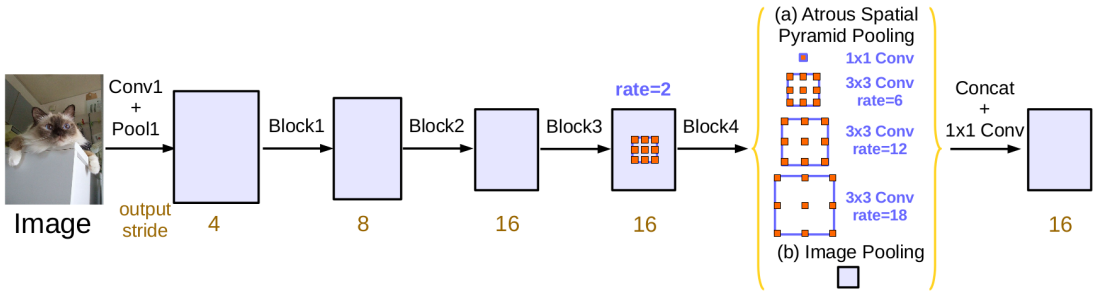

(b) ASPP module in DeepLabv3

Figure 5.4: Illustration of two different context modules used in deepLabv3.

5.4 DeepLabv3+

DeepLabv3+ is designed to combine the ability of ASPP module which can capture rich context information and the ability of encoder-decoder networks which can produce sharp object boundary delineation. Xception, mobileNetv2 and ResNet-101 are used as encoders out of which this work only considers xception and mobileNetv2 for their resource efficiency. The major differences in deepLabv3+ is the use of a decoder, the use of atrous separable convolutions in both the encoder and decoder and the adaption of mobileNet and xception as network backbones (encoders).

The authors call the ratio of input resolution to the output resolution before global average pooling as the output stride. DeepLabv3 is designed to have an output stride of 16. To bring the prediction to the original image resolution, the final features are upsampled by using bilinear interpolation by a factor of 16. This

is considered by the authors as a naive decoder module. Instead of this naive approach, the authors propose the use of a better decoder module. The final encoder features are first upsampled by a factor of 4, and are concatenated with the low level features from the encoder with same dimensions. The number of channels in the low level features are first reduced using a 1×1 convolution. A 3×3 convolution convolves over this concatenated features to refine the features and is later followed by an upsampling of 4 to lead to the final prediction. The architecture of deepLabv3+ is depicted in 5.5.

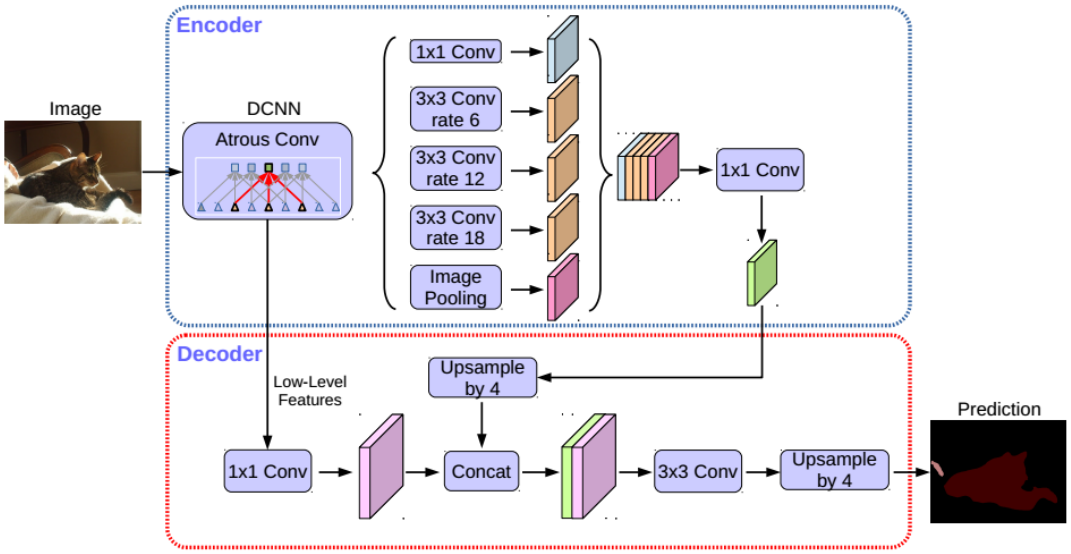

Figure 5.5: An illustration of deepLabv3+ architecture. The encoder extracts features at different scales and the decoder refines object boundary delineation.

The mobileNetv2 and xception encoders make use of depthwise separable convolutions to improve resource efficiency. Sections 5.5 and 5.6 provide details regarding mobileNetv2 and xception architectures respectively. In deepLabv3+, the authors use atrous convolution instead of depthwise convolution in depthwise seperable convolution. The authors call this type of convolutions as atrous separable convolution and state that these convolutions can be used to extract feature maps at arbitrary resolution. The authors use a modified version of the xception architecture as depicted in 5.6 as one of the network backbones.

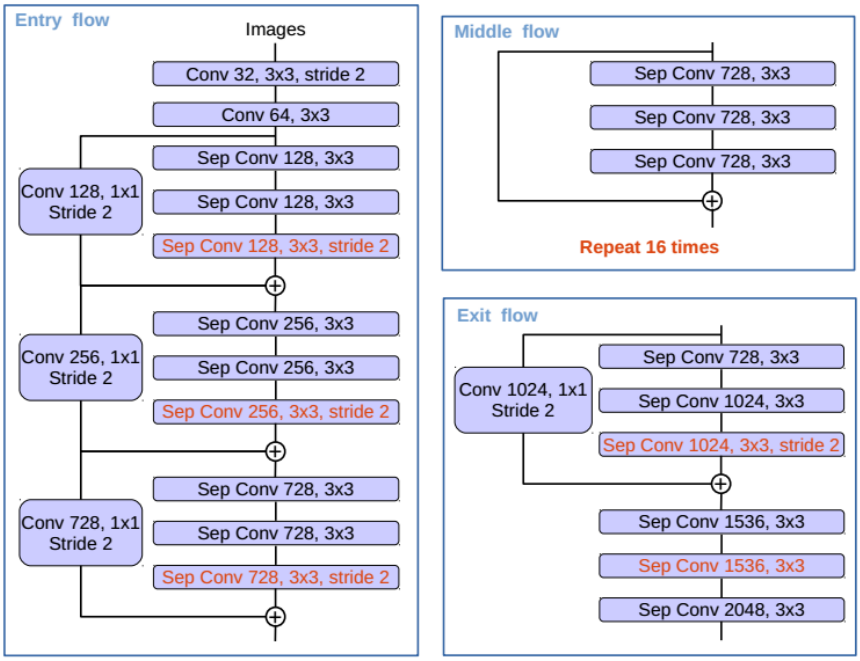

Figure 5.6: Modified xception architecture used as encoder in deepLabv3+. The max pooling operations in the original xception architecture are replaced with depthwise separable convolutions. Batch normalization and ReLU activation is applied after each 3×3 depthwise convolution.

5.5 MobileNetv2

The mobileNetv2 architecture is designed to work on mobile and embedded devices where computational resources are limited. The authors state that their main contribution is the use of a novel layer module called the inverted residual with linear bottleneck.

Depthwise separable convolutions, known for its efficiency, is used in this work. Standard convolution layers are replaced with two layers where the first layer performs depthwise convolution and the second layer performs pointwise convolution. A depthwise convolution layer uses a single fiter per input channel to perform convolution. The pointwise convolution layer consists of 1×1 convolutions which perform weighted linear combination on the input channels and project them to a new channel space. This factorization of standard convolution layer into two separate depthwise and pointwise layers leads to roughly k^2 times reduction in

computation cost where k is the kernel size of the convolutional filter. Figure 5.7 illustrates depthwise convolution. In this case, pointwise convolution performs dimensionality reduction as the number of output channels is less than number of input channels. However, in this case, if more than 3 pointwise convolutions are used, dimensionality output channels can be increased.

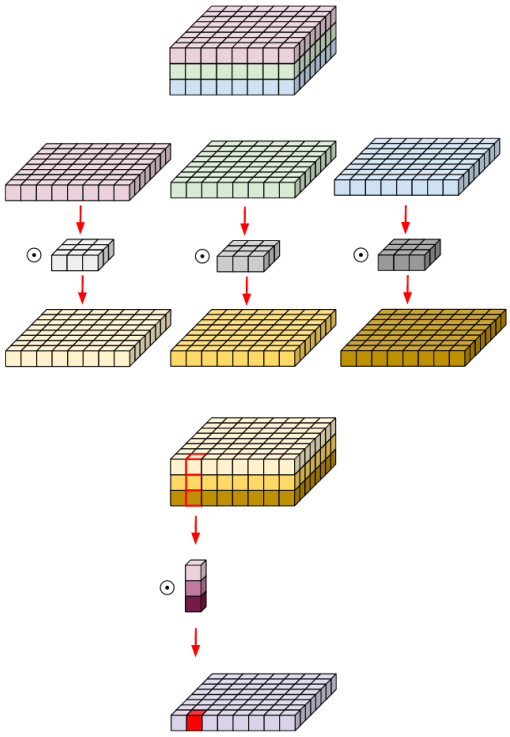

Figure 5.7: An illustration of depthwise separable convolution with 3 input channels and 1 output channel. The first row shows the three input channels. The next three rows illustrate three separate 3×3 convolution convolving over one of the input channels. The fifth row shows the resulting feature maps of the three convolutions being stacked upon each other. Rows 2 to 5 together is the depthwise convolution. The sixth row shows a pointwise convolution convolving over the output of depthwise convolution to get the final output channel

In the original residual block [cite], first a 1×1 convolution is used to reduce the number of channels. On this reduced number of channels 3×3 standard convolution is done which is followed by a 1×1 convolution which now expands the feature maps to have the same number of channels as the input to the block. A skip connection is then introduced through which the input channels is added to the output channels

of the residual block. The skip connection provides a layer with access to earlier activations and also helps prevents the vanishing gradients problem.

The authors of mobileNetv2 propose the use of inverted residual block which takes advantage of the depthwise seperable convolutions. This block consists of a narrow bottleneck layer followed by a 1×1 convolution which performs expansion of number of channels. Depthwise convolution is performed on the expanded input channels followed by a pointwise convolution which brings down the number of channels to create the next bottleneck layer. A skip connection is then added between the input bottleneck and the output bottleneck. The original and inverted residual blocks are depicted in 5.8. The authors use linear activation in the bottleneck layers and hypothesize that it is better than non-linear activation.

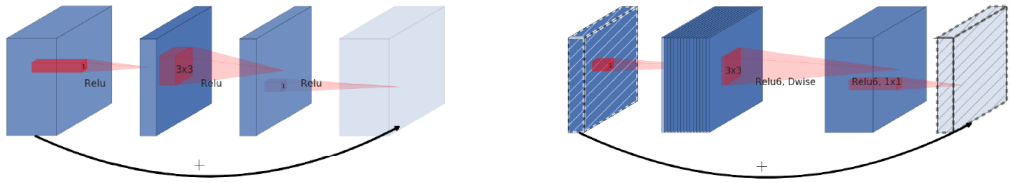

(a) Residual block (b) Inverted residual block

Figure 5.8: Illustration of the original residual block and the inverted residual block used by mobileNetv2.

This hypothesis is based on the notion that the ReLU activation layer used, leads to information loss due to loss of values less than 0. However, loss of too much information due to the induced nonlinearity by the activation can be prevented by the use of linear activation in the bottleneck layer. The authors show that a linear activation is empirically better than a non linear activation in the bottleneck layer.

The inverted residual block has less number of parameters than the residual block and with linear bottleneck is shown to achieve state-of-the-art performance. The inverted residual block is visualized in the architecture of mobileNetv2 in 5.9.

5.6 Xception

The xception architecture is derived based on two hypothesis made by the authors. One hypothesis is based on the inception architecture and the other is a stronger version of the inception hypothesis. Standard convolution layers has

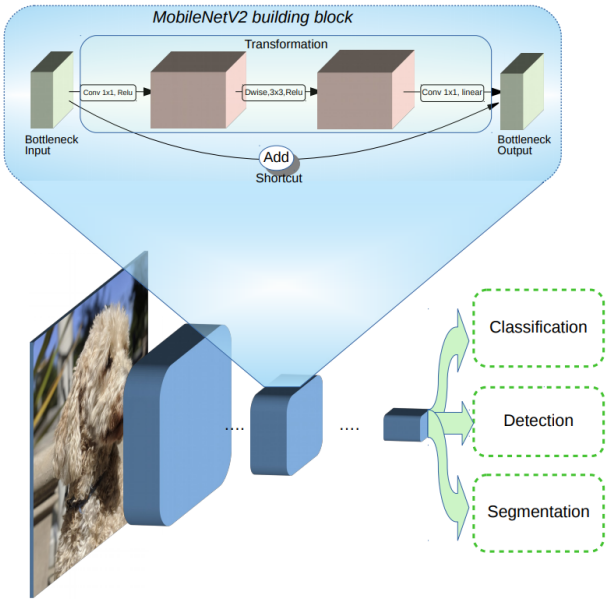

Figure 5.9: The building block of mobileNetv2. The compressed representation obtained could be used for tasks such as image classification, object detection and semantic segmentation.

3D convolution kernals which maps both spatial correlations and cross-channel correlations at the same time. Here spatial correlations is obtained by mapping correlations across the height and the width of every channel separately. Cross-channel correlations is obtained at every spatial location across the height and width of the channels, from each of the channels in the input.

In the inception architecture, an inception module consists of 4 branches operating on the same input feature maps. The different branches of the inceptionv3 module is shown in 5.10a. In the second branch with 1×1 convolution followed by a 3×3 convolution, the 1×1 convolution calculates the cross-channel correlation between the input channels and performs dimensionality reduction by reducing the number of input channels. Next, the 3×3 convolution is a standard convolution which looks for both spatial and cross-channel correlations in this reduced input channel space. Since this inception module has lead to state-of-the-art classification results, the authors hypothesize that the cross-channel correlations and spacial correlations are decoupled and can be mapped separately. This is evidently based on the fact that the inception module partially handles spatial and cross-channel

correlations in a decoupled fashion by using a 1×1 convolution followed by a 3×3 convolution.

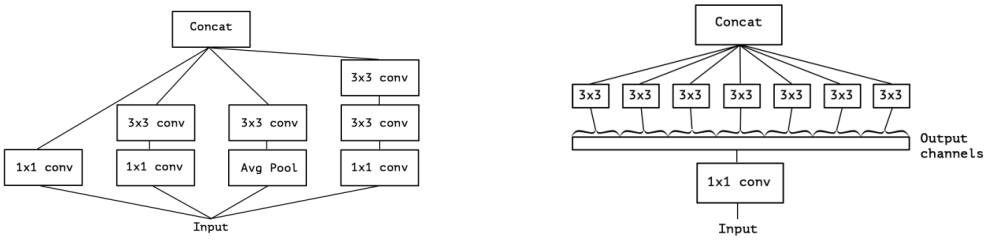

(a) Inceptionv3 module

(b) Extreme version of inception module

Figure 5.10: Illustration of the inception v3 module and an extreme version of the inception module. In the extreme version, each of the 3×3 convolution operates on a single output channel of 1×1 convolution.

Based on this hypothesis, the authors propose that the two correlations can be mapped completely independent of each other leading to a stronger hypothesis. An illustration of this stronger hypothesis can be seen in 5.10b. The xception network is based on this stronger hypothesis and is named "xception" as the architecture is a extreme version of inception. The complete decoupling of the two correlations, could be obtained using depthwise separable convolution, as evidently, this type of convolution first performs depthwise convoltion which handles the spatial correlation and then performs pointwise convolution which handles cross-channel correlation.

5.7 Pruning

A trained Deep Convolutional Neural Network (DCNN) might have weights which are redundant in terms of its effect on the performance during inference.

5.8 Quantization

6

Experimental Evaluation

Since the major contribution of this work is the creation of the dataset, the experiments are focused on validating the effectiveness of the dataset.

6.1 Comparing dataset variants

- **Objective**: The objective of this experiment is to compare the performance of deepLabv3+ on the different dataset variants.
- **Expected result**: The segmentation model is expected to perform better when the number of classes is lower. This is based on the notion that when similar objects are considered as different classes, the model would not have sufficient features to distinguish them.
- **Inference from the results**: Deeplabv3+ with both the mobileNetv2 network backbone and the xception network backbone are evaluated on all variants of variety of backgrounds and white backgrounds dataset. From 6.1, it is evident that the mIOU obtained on each variant is dependent on the properties of objects in the variant. The atWork_full variant treats all the 18 objects in the dataset as different classes. As a result, for instance, m20 and m30 have different labels despite the fact that the two objects only differ in size and slightly in color. The segmentation model is thus forced to distinguish between such objects. Since the objects occur in the dataset at arbitrary scales and are subject to differences in illumination, the real world

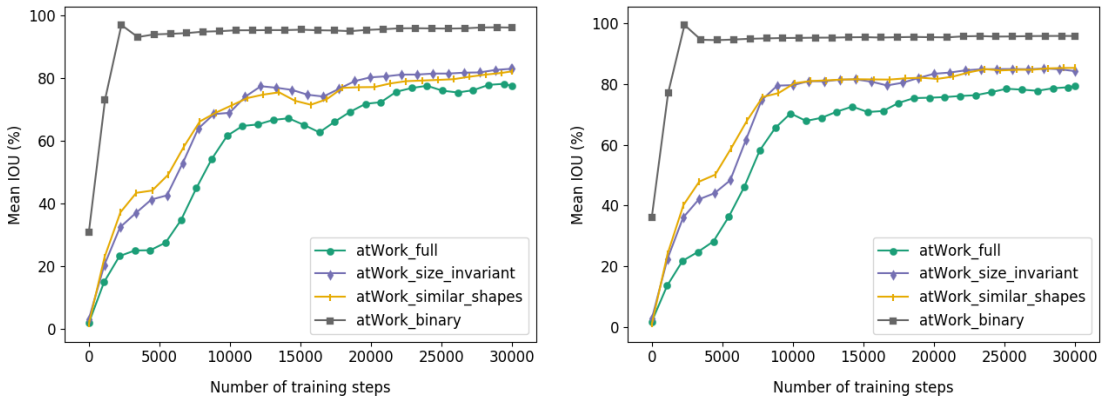

(a) (b)

Figure 6.1: mIOU of deeplabv3+ with **mobileNet network backbone** on variety of backgrounds dataset and white backgrounds dataset is shown. (a) mIOU on the 4 variants of the variety of backgrounds dataset: atWork_full = 77.47%, atWork_size_invariant = 83.10%, atWork_similar_shapes = 82.10% and atWork_binary = 96.06%. (b). mIOU on the 4 variants of the white backgrounds dataset: atWork_full = 79.26%, atWork_size_invariant = 84.29%, atWork_similar_shapes = 85.33% and atWork_binary = 95.83%.

differences between such similar objects become insignificant in the dataset. Thus, the mIOU obtained in the atWork_full variant is indeed the lowest as expected. The two variants atWork_size_invariant and atWork_similar_shapes combine objects which are similar. As a result, the segmentation model achieves better mIOU on these variants. The atWork_binary variant requires the segmentation model to only distinguish foreground from background leading to the highest mIOU. From 6.2, deepLabV3+ with the xception network backbone, evidently, also follows a similar trend like deepLabv3+ with mobileNetv2 network backbone.

6.2 Comparing deepLabv3+ backbones

- **Objective**: The objective of this experiment is to compare the mIOUs obtained by deepLabv3+ with mobileNet and xception network backbones on each of the datasets and its variants.

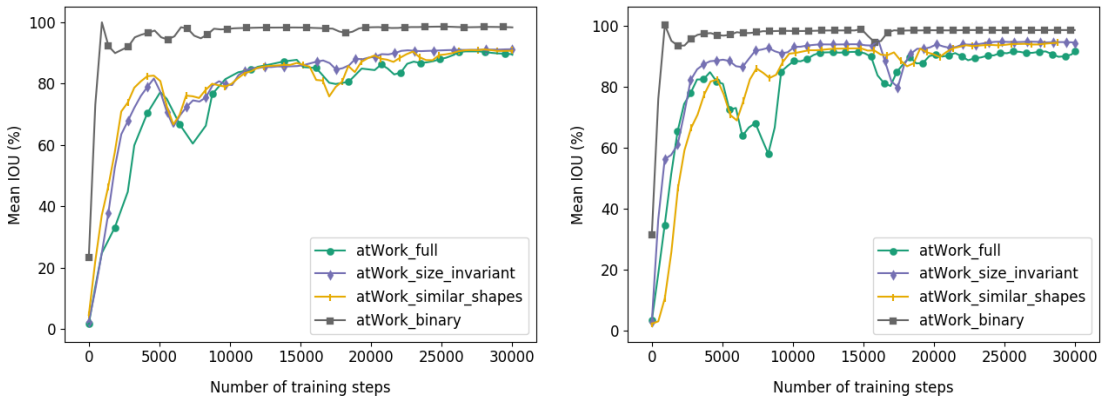

(a) (b)

Figure 6.2: mIOU of deeplabv3+ with **xception network backbone** on variety of backgrounds dataset and white backgrounds dataset is shown. (a). mIOU on the 4 variants of the variety of backgrounds dataset: atWork_full = 89.38%, atWork_size_invariant = 91.19%, atWork_similar_shapes = 90.81% and atWork_binary = 98.31%. (b). mIOU on the 4 variants of the white backgrounds dataset: atWork_full = 91.59%, atWork_size_invariant = 94.27%, atWork_similar_shapes = 94.33% and atWork_binary = 98.47%.

- **Expected result**: The xception network backbone is expected to obtain higher mIOU because of the higher number of learnable parameters in comparison with the mobileNet network backbone. In essence, the xception network backbone has more "learning capacity" than the mobileNet network backbone leading to the ability to learn a better decision boundary.

- **Inference from the results**: Across all the dataset variants, the xception network backbone achieves higher mIOU than the mobileNet network backbone consistently. Another inference is that the models trained and validated on the white backgrounds dataset perform slightly better than corresponding models trained on variety of backgrounds dataset. This supports the notion that it is easier to distinguish the atWork objects when the image background is predominantly white.

6.3 Training with different data

- **Objective**: The objective of this experiment is to assess the effectiveness of the created artificial data. On this regards, starting from the same initial weights, deepLabv3+ with each of the two network backbones is trained on:

  1 Entire training set of the variety of backgrounds dataset consisting of both real and artificial images.

  2 Only the artificial images in the training set of variety of backgrounds dataset.

  3 Entire training set of the white backgrounds dataset consisting of both real and artificial images.

  4 Only the real training images.

  The validation set only consists of the real validation images in order to consider only real world conditions.

- **Expected result**: Training with the entire training set of the variety of backgrounds dataset is expected to achieve the highest mIOU. This is based on the notion that the artificial images forces the segmentation model to learn

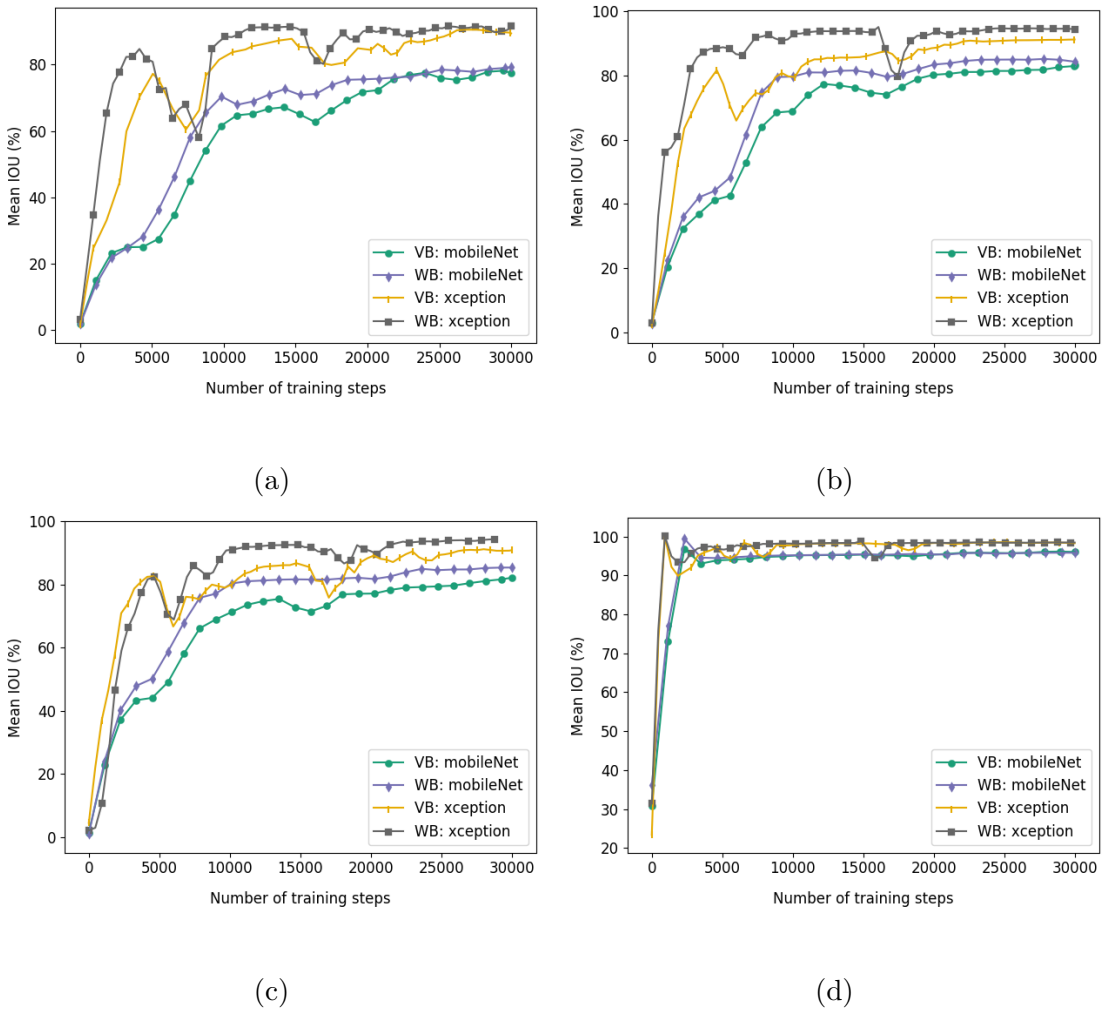

Figure 6.3: Comparison of mIOU obtained by deepLabv3+ using mobileNet network backbone vs xception network backbone on all 4 variants. VB denotes variety of backgrounds dataset and WB denotes white backgrounds dataset. The dataset variant is (a): atWork_full variant, (b): atWork_size_invariant, (c): atWork_similar_shapes and (d): atWork_binary.

features independent of the background. Also, the model is expected to have improved robustness towards varying object scales and occlusions. Training with just the real training images is also expected to perform well but second to the performance obtained with the entire variety of backgrounds training set. Training with white backgrounds dataset is expected to perform well except in cases where the background is not predominantly white. Training only with the artificial images is expected to perform the worst as it does not introduce the segmentation model to real world conditions.

- **Inference from the results**: The results show that in all variants, training with just the real images achieves the best mIOU on the real validation set. This is in contrast to the notion that augmenting with artificial images improves mIOU. This apparent contrast begs to question the need for artificial images and states that they are not required. However, looking into the limitations of the real validation set could help reinstate the importance of the artificial images.

  1 The real validation images only contain one object per image which in most images is clearly visible. There is no cases of occlusion or existance of multiple objects.

  2 The backgrounds in the real validation set is already seen in the training set. Only three different real backgrounds were used.

  These two limitations exist in the real validation because of the need to reduce the labeling cost. Creating real world variations in terms of multiple objects per image and random occlusions is time consuming and also leads to increase in annotation time. Introducing varied backgrounds in real images is also time consuming. These limitations are addressed by the artificial images by placing objects at arbitrary scales in random locations on varied backgrounds. In addition to the existing limitations, the artificial images inherently impose a regularization effect on the training process. This can be attributed to the existence of many different backgrounds. On this regard, the existing L2 regularization weight decay term might need to be lowered to enable the model to better fit to the training data.

Variant	Real training data	Variety of backgrounds all training data	White backgrounds all training data	Variety of backgrounds artificial training data
atWork_full	83.21	71.72	70.8	40.0
atWork_size_invariant	85.01	80.08	77.12	47.76
atWork_similar_shapes	79.83	77.33	76.47	43.31
atWork_binary	94.33	93.01	90.17	43.29

Table 6.1: This table summarizes the results obtained when validating only on the real validation data. The first column denotes the variant. The remaining columns denote on what data was the deepLabv3+ with mobileNet network backbone model trained on. All the mIOUs are in percentage.

Variant	Real training data	Variety of backgrounds all training data	White backgrounds all training data	Variety of backgrounds artificial training data
atWork_full	87.03	80.26	78.42	45.67
atWork_size_invariant	90.84	89.58	87.67	41.58
atWork_similar_shapes	92.85	87.76	83.58	43.32
atWork_binary	98.19	95.21	94.31	47.91

Table 6.2: This table summarizes the results obtained when validating only on the real validation data. The first column denotes the variant. The remaining columns denote on what data was the deepLabv3+ with xception backbone model trained on. All the Mean IOUs are in percentage.

- Suggestions to improve the experiment: Adding a limited number of real validation images which have multiple objects and occlusions, reducing the value of L2 weight decay are two possible changes which can be introduced to arrive at a better inference. However, at this point in order to validate these speculations, model trained only on real data is validated on artificial data. [**result to be attached**] In this case, the mIOU obtained is only around 40 percent proving that this speculation could be further explored.

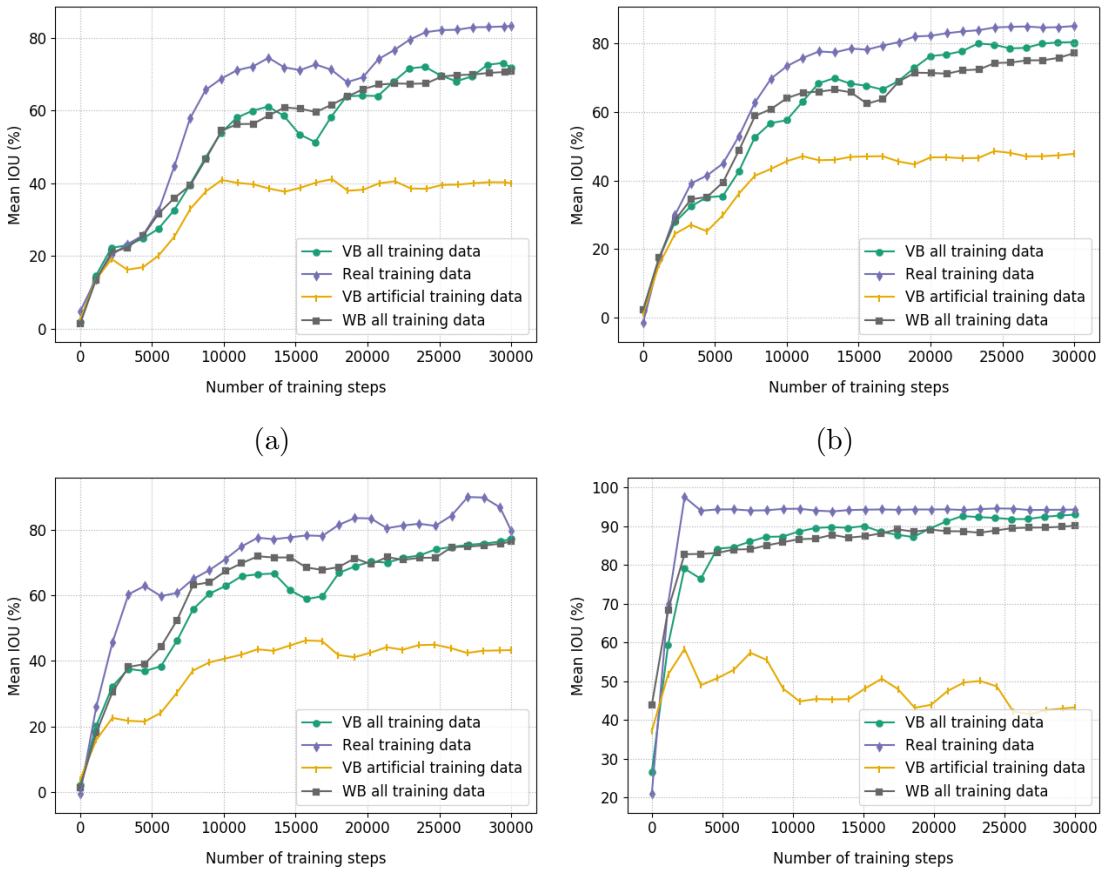

Figure 6.4: mIOU on all 4 variants obtained by deepLabv3+ with mobileNet network backbone when validated only on the real validation data. VB stands for variety of backgrounds dataset and WB stands for white backgrounds dataset. (a): atWork_full, (b): atWork_size_invariant, (c): atWork_similar_shapes and (d): atWork_binary. The Mean IOUs are tabulated in **??**

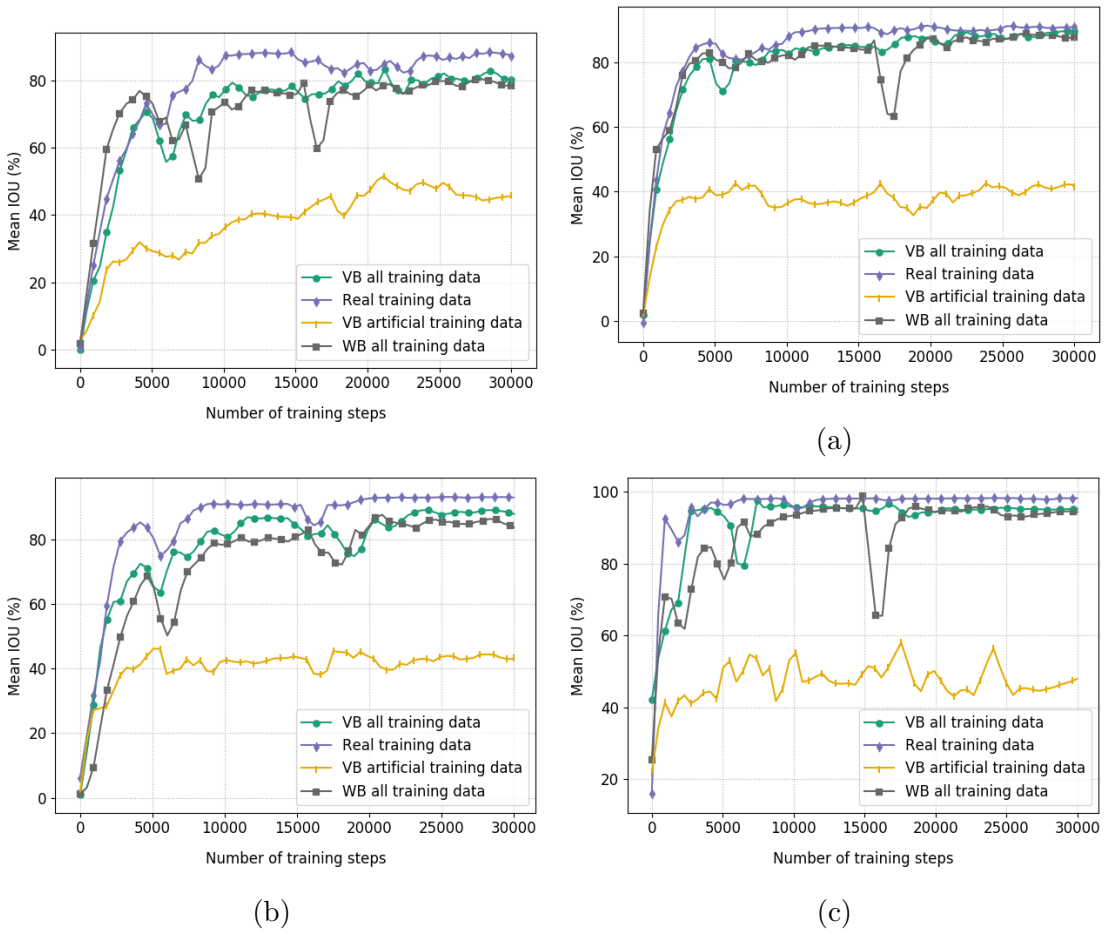

Figure 6.5: mIOU on all 4 variants obtained by deepLabv3+ with xception backbone when validated only on the real validation data. VB stands for variety of backgrounds dataset and WB stands for white backgrounds dataset. (a): atWork_full variant, (b): atWork_size_invariant, (c): atWork_similar_shapes and (d): atWork_binary. The Mean IOUs are tabulated in **??**

6.4 Comparing individual classes

6.4.1 Confusion matrix

- **Objective**: The objective of this section is to analyze the deepLabv3+ models inability to distinguish between different objects.

- **Expected result**: The variants with higher number of classes is expected to have more non leading diagonal terms in the confusion matrix. This is based on the belief that the segmentation model would face difficulties distinguishing objects very similar to each other. This problem is expected to be alleviated by the atWork_size_invariant and atWork_similar_shapes variants. On the atWork_binary variant, there is a possibility that a certain percentage of foreground pixels are confused with background.

- **Inference from the results**: On all the confusion matrices, the leading diagonal elements have highest values in each row. This is expected and suggests that the model correctly classifies a majority of pixels in each class. Notably, the objects confused with each other are either similar in terms of color or shape. For instance, around 10 percent of m30 is confused as m20. This is reasonable as the objects are similar in shape and only differ in size. The difference in size cannot be picked up by the model as no consistent information regarding the object size is available in the dataset. 41.18 percent of pixels in distance tube are confused with background. This could be because the number of pixels occupied by distance tube in the dataset is small in comparison to the other objects. Confusions between objects has reduced on the atWork_size_invariant and atWork_similar_shapes dataset in comparison to the atWork_full variant. This can be attributed to the combining of similar objects to one class. The confusion between motor and m20_100 and the confusion between motor and r20 needs to be addressed.

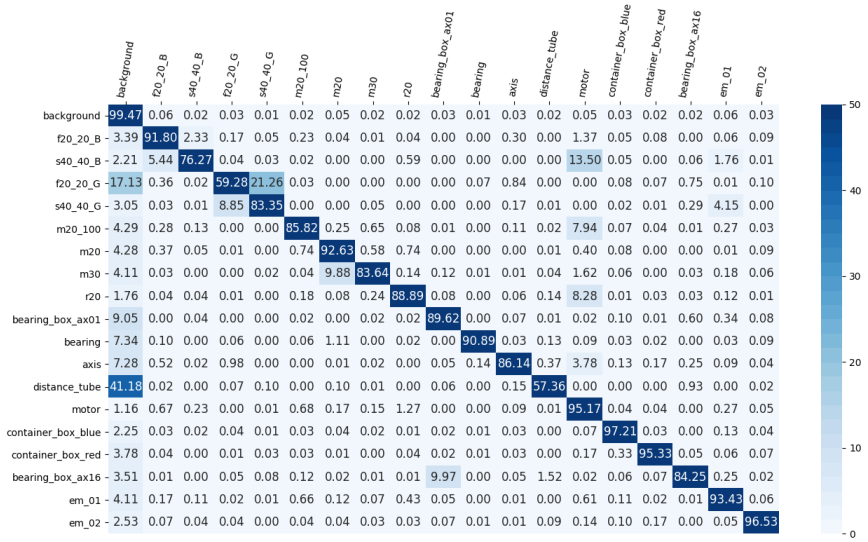

(a)

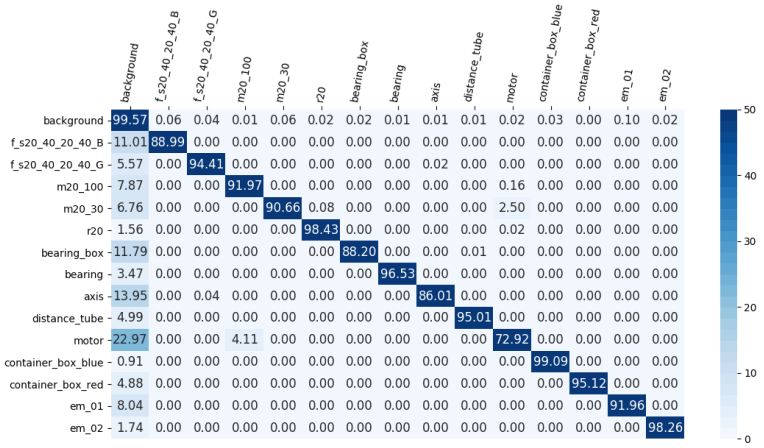

(b)

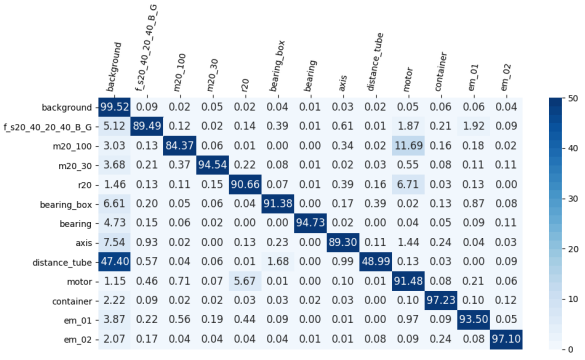

(c)

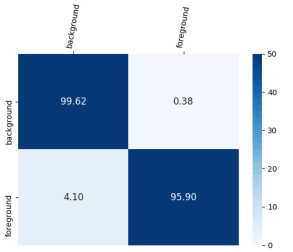

(d)

Figure 6.6: Confusion matrix of deepLabv3+ with mobileNet backbone based on number of classified pixels on all 4 variants of the variety of backgrounds dataset. The number of pixels in each row is normalized by the total number of pixels in the row. (a): atWork_full variant, (b): atWork_size_invariant, (c): atWork_similar_shapes and (d): atWork_binary.

6.4.2 Class IOUs

- **Objective**: The objective of this experiment is to look for a relationship between the individual class IOUs and the percentage of pixels occupied by each class in the dataset.

- **Expected result**: With increase in percentage of pixels, the class IOU is expected to increase. This is based on the notion that the segmentation model gives preference to objects which dominate the dataset.

- **Inference from the results**: For each class, the mean over 30000 training steps of class IOU is calculated. Both the percentage of pixels and the class IOU is normalized with respect to the maximum value out of all objects. The classes are arranged in increasing order of percentage of pixels. The plots are shown in 6.7. From the lower histogram plot for atWork_full variant shown in 6.7a, the class IOUs denoted by the green bars do not seem to show an increasing trend. However, when every 3 classes starting from class distance_tube are combined and plotted separately, (shown in the upper graph of 6.7a). Similar observations can be made for the other two variants as shown in 6.7b and 6.7c. Another interesting result is that the segmentation model seems to learn the object "bearing" well despite the fact that the object only occupies few pixels in the dataset. This could be because of the distinct black ring in between two silver rings present in the bearing. This pattern seems unique and the model probably picks up this pattern with ease.

6.5 Comparing learning rate policies

- **Objective**: The objective of this experiment is to compare the cosine restarts [**needs reference**] learning rate policy with the poly learning rate policy used by deepLabv3+.

- **Expected result**: Either of the two learning rate policies is expected to result in better Mean IOU.

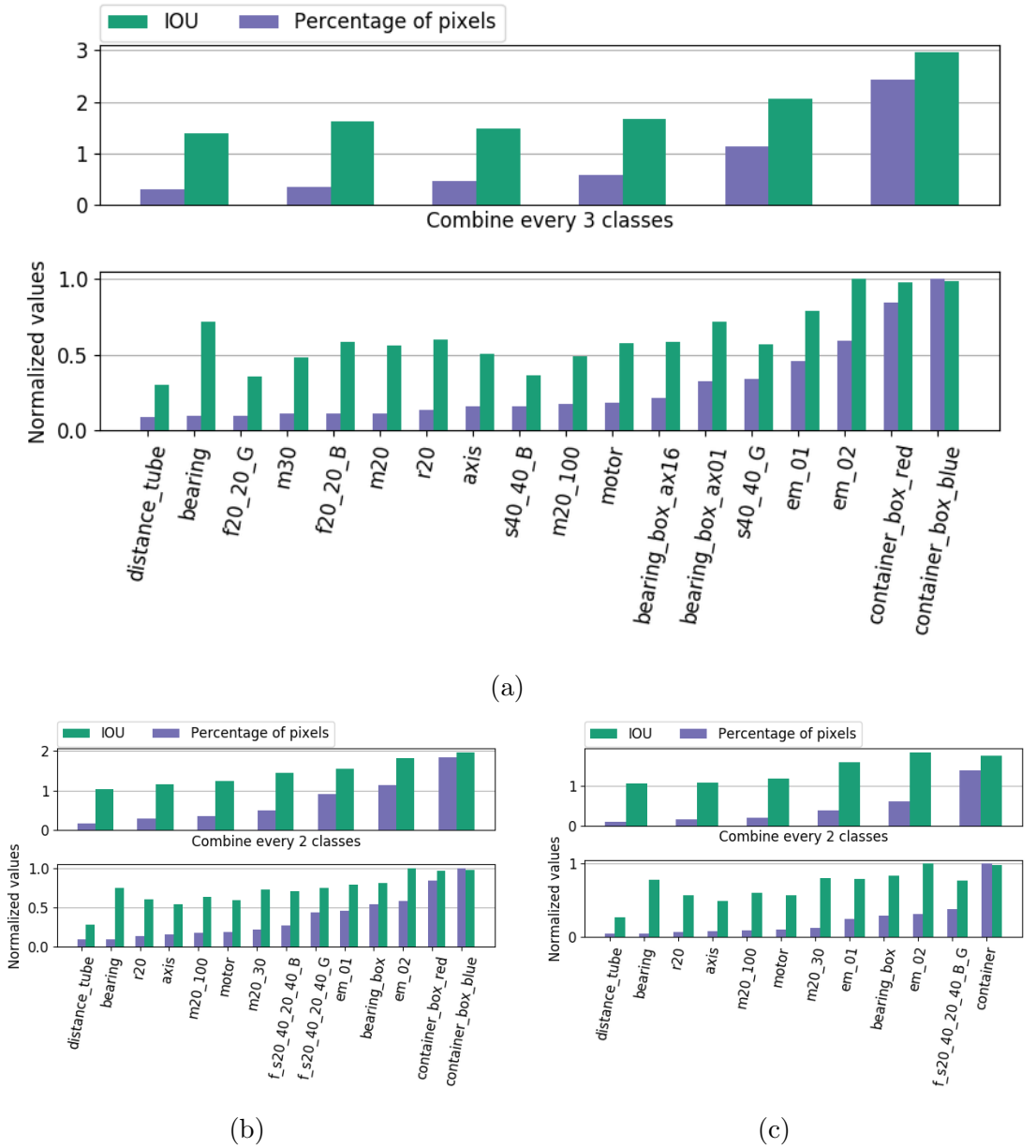

Figure 6.7: Individual class IOUs achieved by deepLabv3+ with mobileNet backbone is plotted with the percentage of pixels occupied on all 4 variants of the variety of backgrounds dataset. The number of pixels in each row is normalized by the total number of pixels in the row. (a): atWork_full variant, (b): atWork_size_invariant, and (c): atWork_similar_shapes.

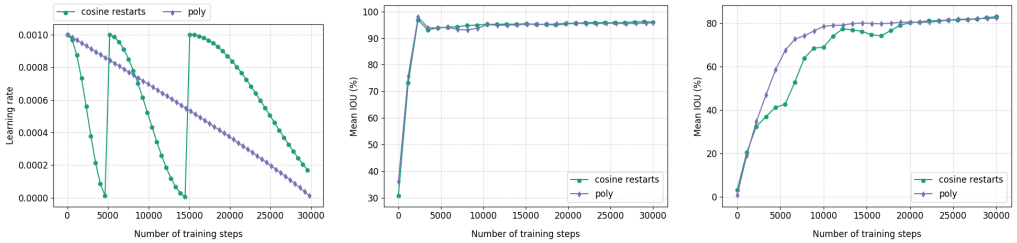

(a) (b) (c)

Figure 6.8: Learning rate decay with two different policies 1. cosine restarts and 2. poly is compared. (a): learning rate over 30000 steps with the two decay policies. (b): Mean IOU on the validation set of atWork_binary variant is 96.06 % with cosine restarts and 95.75 % with poly. (c): Mean IOU on the validation set of atWork_size_invariant variant is 83.1 % with cosine restarts and 82.24 % with poly.

- **Inference from the results**: DeepLabv3+ with mobileNet backbone is used for this experiment. Evidently, the cosine restart learning rate policy leads to slightly better Mean IOU on both the atWork_binary and the atWork_size_invariant variants.

6.6 Effects of class balancing

- **Objective**: The objective of this experiment is to prevent the deepLabv3+ model from giving preference to dominant classes in the dataset. A weight coefficient is determined for each class based on the percentage of pixels occupied by the class in the dataset. These weight coefficients are multiplied with the loss term of the corresponding class in the loss function.

- **Expected result**: The model is expected to achieve similar class IOUs on all the objects. The overall Mean IOU is also expected to be comparable to the Mean IOU obtained without class balancing.

- **Inference from the results**:

6.7 Effects of quantizing the inference graph

- **Objective**: The objective of this experiment is to compare a model with floating point weights and the corresponding model with fixed point weights in terms of Mean IOU, occupied disk memory and inference time.

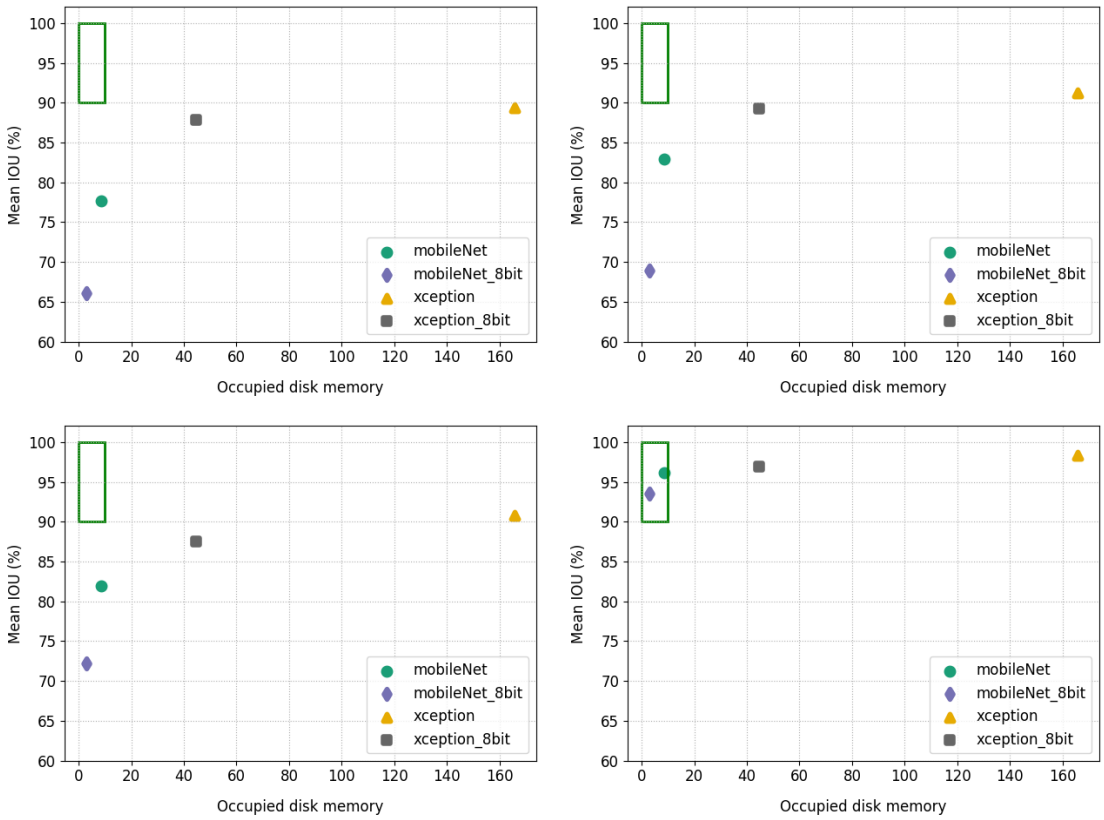

Figure 6.9: .

- **Expected result**:
- **Inference from the results**:

6.8 Transfer learning

- **Objective**:
- **Expected result**:
- **Inference from the results**: Size invariant;mobileNet: PASCAL VOC 2012 = 83.1, mobileNet: atWork_binary = 83.26, xception: PASCAL VOC 2012 = 91.19, xception: atWork_binary = 92.14...Similar shapes;mobileNet: PASCAL VOC 2012 = 82.1, mobileNet: atWork_binary = 82.8, xception: PASCAL

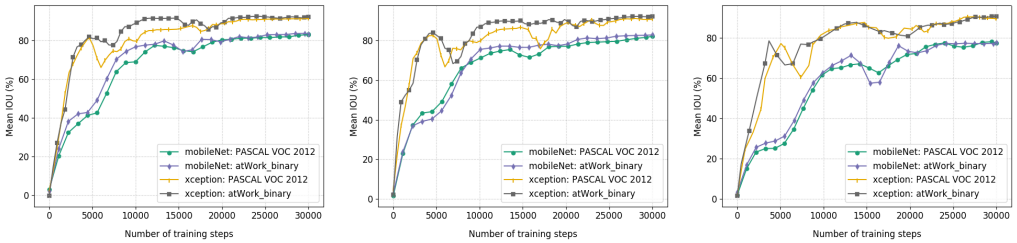

(a) (b) (c)

Figure 6.10: Mean IOU for 30,000 training steps obtained on three variants by deepLabv3+ with xception and mobileNetv2 as network backbones when pretrained on either PASCAL VOC 2012 dataset or atWork_binary variant. As expected, pretrained weights from atWork_binary variant leads to a better Mean IOU. The figures show the results on variants of the variety of backgrounds dataset: (a) atWork_size_invariant, (b) atWork_similar_shapes, (c) atWork_full.

VOC 2012 = 90.81, xception: atWork_binary = 92.15...Full;mobileNet: PASCAL VOC 2012 = 77.47, mobileNet: atWork_binary = 77.73, xception: PASCAL VOC 2012 = 89.38, xception: atWork_binary = 90.64

7

Conclusions

7.1 Contributions

7.2 Lessons learned

7.3 Future work

A

Design Details

Your first appendix

B

Parameters

Your second chapter appendix

References

[1] github: robocup-at-work/rulebook/images; link: https://github.com/robocup-at-work/rulebook/tree/master/images. URL https://github.com/robocup-at-work/rulebook/tree/master/images.

[2] githib: hardikvasa/google-images-download; link: https://github.com/hardikvasa/google-images-download.

[3] List of 20 simple, distinct colors; link: https://sashat.me/2017/01/11/list-of-20-simple-distinct-colors/. URL https://sashat.me/2017/01/11/list-of-20-simple-distinct-colors/.

[4] Liang-Chieh Chen, Yukun Zhu, George Papandreou, Florian Schroff, and Hartwig Adam. Encoder-decoder with atrous separable convolution for semantic image segmentation. *CoRR*, abs/1802.02611, 2018. URL http://arxiv.org/abs/1802.02611.

[5] Kaiming He, Xiangyu Zhang, Shaoqing Ren, and Jian Sun. Deep residual learning for image recognition. *CoRR*, abs/1512.03385, 2015. URL http://arxiv.org/abs/1512.03385.

[6] Author Name. Book title. *Lecture Notes in Autonomous System*, 1001:900–921, 2003. ISSN 0302-2345.

[7] Param S. Rajpura, Manik Goyal, Hristo Bojinov, and Ravi S. Hegde. Dataset augmentation with synthetic images improves semantic segmentation. *CoRR*, abs/1709.00849, 2017. URL http://arxiv.org/abs/1709.00849.

[8] Joseph Redmon, Santosh Kumar Divvala, Ross B. Girshick, and Ali Farhadi. You only look once: Unified, real-time object detection. *CoRR*, abs/1506.02640, 2015. URL http://arxiv.org/abs/1506.02640.

[9] German Ros, Laura Sellart, Joanna Materzynska, David Vazquez, and Antonio Lopez. The SYNTHIA Dataset: A large collection of synthetic images for semantic segmentation of urban scenes. 2016.

[10] Karen Simonyan and Andrew Zisserman. Two-stream convolutional networks for action recognition in videos. *CoRR*, abs/1406.2199, 2014. URL `http://arxiv.org/abs/1406.2199`.